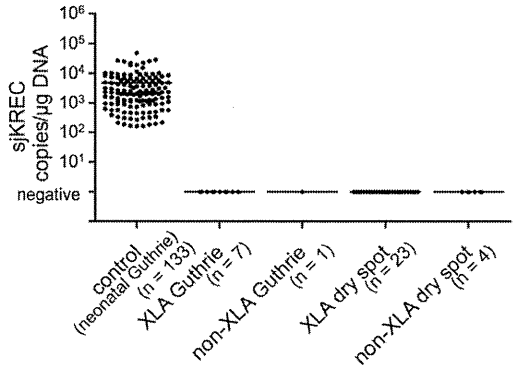

FIG 2. Copy numbers of sjKRECs measured in neonatal Guthrie cards or dried blood spots obtained from B-cell–deficient patients. On all samples from control, neonatal Guthrie cards (n = 133) were sjKREC-positive ($4.8 \pm 0.6 \times 10^3$ copies/μg DNA). B-cell–deficient patients were negative for sjKRECs in neonatal Guthrie cards (XLA, n = 7; non-XLA, n = 1) and dried blood spots (XLA, n = 23; non-XLA, n = 4).

One patient (P27) was positive for cjKRECs, but other patients were negative for it. *RPPH1* (internal control) was detectable at the same level as in normal controls in all samples.

These results indicate that sjKRECs are undetectable in XLA and non-XLA and suggest that measurement of sjKRECs in neonatal Guthrie cards has the potential for the use of newborn mass screening to identify neonates with early B-cell maturation defects. Greater numbers of neonatal Guthrie cards should be examined to confirm this potential, and the data obtained from dried blood spots on filter papers must be examined to prove that they truly reflect the data obtained from neonatal Guthrie cards. We should also examine whether screening can reduce the cost of treatment of the bacterial infections and chronic lung diseases in patients with XLA and non-XLA and increase the benefits for these patients. An anticipated pilot study using a large cohort of newborns must address these problems. We also found that T-cell–receptor excision circles and sjKRECs can be measured simultaneously on the same plate. Thus, a pilot study of neonatal screening for both T-cell and B-cell deficiencies could be performed simultaneously.

We thank the patients and their families who participated in this study. We also thank Ms Makiko Tanaka and Ms Kimiko Gasa for their skillful technical assistance and members of the Department of Obstetrics and Gynecology at the National Defense Medical College for collecting umbilical cord blood samples as well as Drs Wataru and Masuko Hirose. We are also indebted to Prof J. Patrick Barron, Chairman of the Department of International Medical Communications of Tokyo Medical University, for his *pro bono* linguistic review of this article.

Noriko Nakagawa, MD[a]
Kohsuke Imai, MD, PhD[a,b]
Hirokazu Kanegane, MD, PhD[c]
Hiroki Sato, MS[b]
Masafumi Yamada, MD, PhD[d]
Kensuke Kondoh, MD, PhD[e]
Satoshi Okada, MD, PhD[f]
Masao Kobayashi, MD, PhD[f]
Kazunaga Agematsu, MD, PhD[g]
Hidetoshi Takada, MD, PhD[h]
Noriko Mitsuiki, MD[i,j]
Koichi Oshima, MD[j,k]
Osamu Ohara, PhD[j]
Deepti Suri, MD[l]
Amit Rawat, MD[l]
Surjit Singh, MD[l]
Qiang Pan-Hammarström, MD, PhD[m]
Lennart Hammarström, MD, PhD[m]
Janine Reichenbach, MD[n]
Reinhard Seger, MD[n]
Tadashi Ariga, MD, PhD[d]
Toshiro Hara, MD, PhD[h]
Toshio Miyawaki, MD, PhD[c]
Shigeaki Nonoyama, MD, PhD[a]

From [a]the Department of Pediatrics, National Defense Medical College, and [b]the Department of Medical Informatics, National Defense Medical College Hospital, Saitama, Japan; [c]the Department of Pediatrics, University of Toyama, Toyama, Japan; [d]the Department of Pediatrics, Hokkaido University, Hokkaido, Japan; [e]the Department of Pediatrics, St Marianna University School of Medicine, Kanagawa, Japan; [f]the Department of Pediatrics, Hiroshima University, Hiroshima, Japan; [g]the Department of Pediatrics, Shinshu University, Nagano, Japan; [h]the Department of Pediatrics, Kyushu University, Fukuoka, Japan; [i]the Department of Pediatrics, Tokyo Medical and Dental University, Tokyo, Japan; [j]the Department of Human Genome Technology, Kazusa DNA Research Institute, Chiba, Japan; [k]the Department of Clinical Application, Center for iPS Cell Research and Application, Kyoto University, Kyoto, Japan; [l]the Advanced Pediatric Centre Post Graduate Institute of Medical Education and Research, Chandigarh, India; [m]the Division of Clinical Immunology, Department of Laboratory Medicine, Huddinge Hospital, Karolinska Institute, Stockholm, Sweden; and [n]the Department of Immunology/Hematology/BMT, University Children's Hospital Zurich, Zurich, Switzerland. E-mail: kimai@ndmc.ac.jp.

Supported in part by grants from the Ministry of Defense; the Ministry of Health, Labor, and Welfare; the Ministry of Education, Culture, Sports, Science and Technology; and the Kawano Masanori Foundation for Promotion of Pediatrics.

Disclosure of potential conflict of interest: The authors have declared that they have no conflict of interest.

REFERENCES

1. Conley ME, Broides A, Hernandez-Trujillo V, Howard V, Kanegane H, Miyawaki T, et al. Genetic analysis of patients with defects in early B-cell development. Immunol Rev 2005;203:216-34.
2. Kanegane H, Futatani T, Wang Y, Nomura K, Shinozaki K, Matsukura H, et al. Clinical and mutational characteristics of X-linked agammaglobulinemia and its carrier identified by flow cytometric assessment combined with genetic analysis. J Allergy Clin Immunol 2001;108:1012-20.
3. Plebani A, Soresina A, Rondelli R, Amato GM, Azzari C, Cardinale F, et al. Clinical, immunological, and molecular analysis in a large cohort of patients with X-linked agammaglobulinemia: an Italian multicenter study. Clin Immunol 2002;104:221-30.
4. Siminovitch KA, Bakhshi A, Goldman P, Korsmeyer SJ. A uniform deleting element mediates the loss of kappa genes in human B cells. Nature 1985;316: 260-2.
5. van Zelm MC, Szczepanski T, van der Burg M, van Dongen JJ. Replication history of B lymphocytes reveals homeostatic proliferation and extensive antigen-induced B cell expansion. J Exp Med 2007;204:645-55.
6. Eades-Perner AM, Gathmann B, Knerr V, Guzman D, Veit D, Kindle G, et al. ESID Registry Working Party. The European internet-based patient and research database for primary immunodeficiencies: results 2004-06. Clin Exp Immunol 2007; 147:306-12.
7. Morinishi Y, Imai K, Nakagawa N, Sato H, Horiuchi K, Ohtsuka Y, et al. Identification of severe combined immunodeficiency by T-cell receptor excision circles quantification using neonatal Guthrie cards. J Pediatr 2009;155:829-33.
8. Ozyurek E, Cetintas S, Ceylan T, Ogus E, Haberal A, Gurakan B, et al. Complete blood count parameters for healthy, small-for-gestational-age, full-term newborns. Clin Lab Haematol 2006;28:97-104.
9. Comans-Bitter WM, de Groot R, van den Beemd R, Neijens HJ, Hop WC, Groeneveld K, et al. Immunophenotyping of blood lymphocytes in childhood: reference values for lymphocyte subpopulations. J Pediatr 1997;130:388-93.
10. Kaneko H, Kawamoto N, Asano T, Mabuchi Y, Horikoshi H, Teramoto T, et al. Leaky phenotype of X-linked agammaglobulinaemia in a Japanese family. Clin Exp Immunol 2005;140:520-3.

Available online March 11, 2011.
doi:10.1016/j.jaci.2011.01.052

TABLE E1. Characteristics of patients with XLA

Patient no.	Unique patient no.	Age (y)	Sex	Serum Ig (mg/dL)			$CD19^+$		*BTK* mutation			Source	
				IgG	IgA	IgM	% Lymph	/μL	Genomic DNA	cDNA	Amino acid	Guthrie	Dry spot
P1	670	0	M	87	<6	10	0.21	12.99	29269G>T	1178-1G>T	Splice acceptor defect	x	
P2	718	0	M	215	<10	<10	0.07	7.04	11593_11594 insA	144_145insA	Arg49 frameshift	x	
P3	722	0	M	80	<1	1	<1.00	NA	25644C>T	763C>T	Arg255X	x	
P4	727	8	M	295	59	57	0.11	3.52	29269G>T	1178-1G>T	Splice acceptor defect		x
P5	732	34	M	1140*	<6	8	0.02	0.24	11631T>A	182T>A	Ile61Asn		x
P6	811	24	M	458*	0	13	0.50	5.32	23570T>G	426T>G	Tyr142X		x
P7	813	18	M	628*	109	6	0.60	6.87	23570T>G	426T>G	Tyr142X		x
P8	814	19	M	260	0	NA	0.20	3.01	16180C>T	344C>T	Ser115Phe		x
P9	815	13	M	600*	<10	<5	0.08	1.72	11590G>T	142-1G>T	Splice acceptor defect		x
P10	816	11	M	12	0	5	0.00	0.00	150kb deletion of *BTK, TIMM8A, TAF7L, DRP2*				x
P11	817	10	M	10	2	24	0.80	35.78	36288C>T	1928C>T	Thr643Ile		x
P12	824	13	M	462	6	27	0.41	14.49	27518C>A	895-11C>A	Splice acceptor defect		x
P13	834	5	M	<237	<37	43	0.00	0.00	25715_26210del	776+57_839+73del	Exon 9 deletion		x
P14	838	21	M	<50	<5	7	0.00	0.00	31596G>C	1631+1G>C	Splice donor defect		x
P15	839	16	M	604*	<1	<2	0.04	0.66	31596G>C	1631+1G>C	Splice donor defect		x
P16	847	11	M	698*	26	11	0.08	1.86	25536delG	655delG	Val219 frameshift		x
P17	877	14	M	20	19	8	0.21	NA	32357T>C	1750+2T>C	Splice donor defect		x
P18	880	5	M	233	39	41	0.06	NA	10941-?_14592+?del	1-?_240+?del	Exon 1-3 deletion		x
P19	888	8	M	<212	<37	150	0.15	6.60	11023G>A	83G>A	Arg28His		x
P20	891	21	M	195	<6	37	0.02	0.09	32243C>G	1638C>G	Cys502Trp		x
P21	958	0	M	<50	<10	9	0.80	27.14	31544_31547 delGTTT	1580_1583del GTTT	Cys527 frameshift		x
P22	701	2	M	115	<2	4	0.09	1.99	16172C>A	336C>A	Tyr112X		x
P23	911	0	M	<10	<6	<4	0.00	0.00	29955A>C	1350-2A>C	Splice acceptor defect	x	
P24	937	0	M	60	<2	58	0.00	0.00	11022C>T	82C>T	Arg28Cys	x	
P25	938	0	M	<20	<4	<6	0.00	0.00	36269-?_36778+?del	1909-?_2418+?del	Exon 19 deletion	x	
P26	939	0	M	60	<2	22	0.00	0.00	11022C>T	82C>T	Arg28Cys	x	
P27	890	12	M	<237	<37	<20	0.03	NA	36261G>A	1909-8G>A	Splice acceptor defect		x
P28	944	6	M	12	<1	1	0.02	NA	36281C>T	1921C>T	Arg641Cys		x
P29	948	5	M	<237	<37	<20	0.01	0.70	36261G>A	1909-8G>A	Splice acceptor defect		x
P30	1053	5	M	386	5	113	1.10	34.22	32259A>C	1654A>C	Thr552Pro		x

Age, Age at analysis of KRECs; *$CD19^+$ % Lymph,* CD19-positive cell percentage in lymphocytes; *$CD19^+$ /μL,* CD19-positive cell number in 1 μL whole peripheral blood; *M,* male; *NA,* not available; *Serum Ig,* serum levels of immunoglobulins at diagnosis.

BTK mutation's reference sequences are NCBI NC_000023.9, NM_000061.2, and NP_000052.1.

*Trough level during intravenous immunoglobulin therapy.

TABLE E2. Characteristics of patients with non-XLA

				Serum Ig (mg/dL)			$CD19^+$			Source	
Patient no.	Unique patient no.	Age (y)	Sex	IgG	IgA	IgM	% Lymph	/μL	*BTK* mutation	Guthrie	Dry spot
P31	596	4	F	386	<6	6	0.42	21.27	Normal		x
P32	719	0	F	<50	<5	<5	0.00	0.00	Normal	x	
P33	835	8	M	311	323	20	0.09	1.88	Normal		x
P34	915	0	M	<212	<37	<20	0.00	0.00	Normal		x
P35	947	0	M	<21	<37	<39	0.00	0.00	Normal		x

Age, Age at analysis of KRECs; *$CD19^+$ % Lymph,* CD19-positive cell percentage in lymphocytes; *$CD19^+$ /μL,* CD19-positive cell number in 1 μL whole peripheral blood; *F,* female; *M,* male; *Serum Ig,* serum levels of immunoglobulins at diagnosis.

A Novel Serum-Free Monolayer Culture for Orderly Hematopoietic Differentiation of Human Pluripotent Cells via Mesodermal Progenitors

Akira Niwa[1,2], Toshio Heike[2], Katsutsugu Umeda[2,4], Koichi Oshima[1], Itaru Kato[1,2], Hiromi Sakai[5], Hirofumi Suemori[3], Tatsutoshi Nakahata[1,2], Megumu K. Saito[1,2]*

1 Clinical Application Department, Center for iPS Cell Research and Application, Kyoto University, Kyoto, Japan, **2** Department of Pediatrics, Graduate School of Medicine, Kyoto University, Kyoto, Japan, **3** Laboratory of Embryonic Stem Cell Research, Stem Cell Research Center, Institute for Frontier Medical Sciences, Kyoto University, Kyoto, Japan, **4** Institute of Molecular Medicine, University of Texas Health Science Center, Houston, Texas, United States of America, **5** Waseda Bioscience Research Institute in Helios, Singapore

Abstract

Elucidating the *in vitro* differentiation of human embryonic stem (ES) and induced pluripotent stem (iPS) cells is important for understanding both normal and pathological hematopoietic development *in vivo*. For this purpose, a robust and simple hematopoietic differentiation system that can faithfully trace *in vivo* hematopoiesis is necessary. In this study, we established a novel serum-free monolayer culture that can trace the *in vivo* hematopoietic pathway from ES/iPS cells to functional definitive blood cells via mesodermal progenitors. Stepwise tuning of exogenous cytokine cocktails induced the hematopoietic mesodermal progenitors via primitive streak cells. These progenitors were then differentiated into various cell lineages depending on the hematopoietic cytokines present. Moreover, single cell deposition assay revealed that common bipotential hemoangiogenic progenitors were induced in our culture. Our system provides a new, robust, and simple method for investigating the mechanisms of mesodermal and hematopoietic differentiation.

Citation: Niwa A, Heike T, Umeda K, Oshima K, Kato I, et al. (2011) A Novel Serum-Free Monolayer Culture for Orderly Hematopoietic Differentiation of Human Pluripotent Cells via Mesodermal Progenitors. PLoS ONE 6(7): e22261. doi:10.1371/journal.pone.0022261

Editor: Dan Kaufman, University of Minnesota, United States of America

Received January 4, 2011; **Accepted** June 18, 2011; **Published** July 27, 2011

Funding: This work was supported by grants from the Ministry of Education, Culture, Sports, Science, and Technology of Japan (#22790979). The funders had no role in study design, data collection and analysis, decision to publish, or preparation of the manuscript.

Competing Interests: The authors have declared that no competing interests exist.

* E-mail: msaito@kuhp.kyoto-u.ac.jp

Introduction

Because of pluripotency and self-renewal, human embryonic stem (ES) cells and induced pluripotent stem (iPS) cells are potential cell sources for regenerative medicine and other clinical applications, such as cell therapies, drug screening, toxicology, and investigation of disease mechanisms [1,2,3]. iPS cells are reprogrammed somatic cells with ES cell-like characteristics that are generated by introducing certain combinations of genes, proteins, or small molecules into the original cells [4,5,6,7]. Patient-derived iPS cells have facilitated individualized regenerative medicine without immunological or ethical concerns. Moreover, patient- or disease-specific iPS cells are an important resource for unraveling human hematological disorders. However, for this purpose, a robust and simple hematopoietic differentiation system that can reliably mimic in vivo hematopoiesis is necessary.

Mesodermal and hematopoietic differentiation is a dynamic event associated with changes in both the location and phenotype of cells [8,9,10,11]. Some primitive streak (PS) cells appearing just after gastrulation form the mesoderm, and a subset of mesodermal cells differentiate into hematopoietic cell lineages [9,12,13,14,15,16]. Previous studies have accumulated evidence on these embryonic developmental pathways.

The leading methods of blood cell induction from ES/iPS cells employ 2 different systems: monolayer animal-derived stromal cell coculture and 3-dimensional embryoid body (EB) formation. Both methods can produce hematopoietic cells from mesodermal progenitors, and combinations of cytokines can control, to some extent, the specific lineage commitment [1,2,17,18,19,20,21,22,23,24,25,26,27,28]. In the former method, a previous study showed that OP9 stromal cells, which are derived from the bone marrow of osteopetrotic mice, augment the survival of human ES cell-derived hematopoietic progenitors [29]. However, as the stromal cell condition controls the robustness of the system, it can be relatively unstable. Furthermore, the induction of hematopoietic cells from human pluripotent cells on murine-derived cells is less efficient than that from mice cells.

In EB-based methods, hematopoietic cells emerge from specific areas positive for endothelial markers such as CD31 [30,31,32]. Through these methods, previous studies have generated a list of landmark genes for each developmental stage, such as *T* and *KDR* genes for the PS and mesodermal cells, respectively [12,16,17,18,25,28,33,34,35,36], and also have emphasized appropriate developmental conditions consisting of specific microenvironments, signal gradients, and cytokines given in suitable combinations with appropriate timing. For robust and reproducible specification to myelomonocytic lineages of cells, some recent studies have converted to serum-independent culture by using EB formation [37]. However, the difficulty in applying 3-dimensional location information inside EBs prevents substantial increases in

hematopoietic specification efficacy. Additionally, the sphere-like structure of the EB complicates tracking and determination of hematopoietic–stromal cell interactions.

To overcome these issues, we established a novel serum-free monolayer hematopoietic cell differentiation system from human ES and iPS cells. Although there are no reports describing the shift of human ES/iPS cells from primitive to definitive erythropoiesis in a monolayer xeno-cell-free condition, our system can trace the in vitro differentiation of human ES/iPS cells into multiple lineages of definitive blood cells, such as functional erythrocytes and neutrophils. Hematopoietic cells arise via an orderly developmental pathway that includes PS cells, mesoderm, and primitive hematopoiesis.

Materials and Methods

Maintenance of human ES/iPS cells in serum-free condition

Experiments were carried out with the human ES cell lines KhES-1 and KhES-3 (kindly provided by Norio Nakatsuji) and iPS cell lines 201B7 and 253G4 (kindly provided by Shinya Yamanaka). Stable derivatives of ES cells carrying the transgene for green fluorescent protein (GFP) after CAG promoter were also used [38,39]. The ES/iPS cells were maintained on a tissue culture dish (#353004; Becton-Dickinson, Franklin Lakes, NJ) coated with growth factor-reduced Matrigel (#354230; Becton-Dickinson) in mTeSR1 serum-free medium (#05850; STEMCELL Technologies, Vancouver, BC, Canada). The medium was replaced everyday. Passage was performed according to the manufacturer's protocol.

Differentiation of ES/iPS cells

First, undifferentiated ES/iPS cell colonies were prepared at the density of less than 5 colonies per well of a 6-well tissue culture plate (#353046; Becton-Dickinson). When individual colony grew up to approximately 500 μm in diameter, mTeSR1 maintenance medium was replaced by Stemline II serum-free medium (#S0192; Sigma-Aldrich, St. Louis, MO) supplemented with Insulin-Transferrin-Selenium-X Supplement (ITS) (#51500-056; Invitrogen, Carlsbad, CA). This day was defined as day 0 of differentiation. BMP4 (#314-BP-010; R&D Systems, Minneapolis, MN) was added for first 4 days and replaced by $VEGF_{165}$ (#293-VE-050; R&D Systems) and SCF (#255-SC-050; R&D Systems) on day 4. On day 6, the cytokines were again replaced by the haematopoietic cocktail described in the result section. Concentration of each cytokine was as follows: 20 ng/mL BMP4, 40 ng/mL $VEGF_{165}$, 50 ng/mL SCF, 10 ng/mL TPO (#288-TPN-025; R&D Systems), 50 ng/mL IL3 (#203-IL-050; R&D Systems), 50 ng/mL Flt-3 ligand (#308-FK-025; R&D Systems), 50 ng/mL G-CSF (#214-CS-025; R&D Systems), 50 ng/mL complex of IL-6 and soluble IL-6 receptor (FP6) (kindly provided by Kyowa Hakko Kirin Co., Ltd., Tokyo, Japan) and 5 IU/mL EPO (#329871; EMD Biosciences, San Diego, CA). Thereafter, the medium was changed every 5 days.

Antibodies

The primary murine anti-human monoclonal antibodies used for flow cytometric (FCM) analysis are as follows: PE-conjugated anti-SSEA-4 (#330405; BioLegend, San Diego, CA), Alexa Fluor® 647-conjugated anti-TRA-1-60 (#560122; Becton-Dickinson), biotin-conjugated anti-CD140a (#323503; Biolegend), Alexa Fluor® 647-conjugated anti-KDR (#338909; BioLegend), PE-conjugated anti-CXCR4 (#555974; Becton-Dickinson), PE-conjugated anti-CD117 (#313203; BioLegend), PE-conjugated CD34 (#A07776; Beckman Coulter, Brea, CA), FITC-conjugated CD43 (#560978; Becton-Dickinson), and APC-conjugated CD45 (#IM2473; Beckman Coulter). A streptavidin-PE (#554061; Becton Dickinson) was used as secondary antibody against biotin-conjugated primary antibody. The primary antibodies used to immunostain the colonies and floating blood cells included anti-human Oct3/4 (#611203; Becton-Dickinson), T (#sc-101164; Santa Cruz Biotechnology, Santa Cruz, CA), KDR (#MAB3571; R&D Systems), VE-Cadherin (#AF938; R&D Systems), and rabbit anti-pan-human Hb (#0855129; MP Biomedicals, Solon, OH). FITC-conjugated donkey anti-rat antibodies and Cy3-conjugated goat anti-mouse antibodies (Jackson ImmunoResearch Laboratories, Inc., West Grove, PA) were used as secondary antibodies.

Cytostaining

Floating cells were centrifuged onto glass slides by using a Shandon Cytospin 4 Cytocentrifuge (Thermo, Pittsburgh, PA) and analysed by microscopy after staining with May–Giemsa or myeloperoxidase. For immunofluorescence staining, cells fixed with 4% paraformaldehyde were first permeabilized with phosphate-buffered saline containing 5% skimmed milk (Becton–Dickinson) and 0.1% Triton X-100 and then incubated with primary antibodies, followed by incubation with FITC or Cy3-conjugated secondary antibodies. Nuclei were counterstained with 4,6-diamidino-2-phenylindole (DAPI) (Sigma-Aldrich).

Flow cytometric analysis

The adherent cells were treated with Dispase (#354235; Becton-Dickinson) and harvested by gently scraping the culture dish. Aggregated cell structure was chopped by a pair of scissors, processed by GentleMACS (Milteny Biotec, Germany) and then dispersed by 40-μm strainers (#2340; Becton-Dickinson) before staining with antibodies. Dead cells were excluded by DAPI staining. Samples were analysed using a MACSQuant (Milteny Biotec) and FlowJo software (Thermo). Cell sorting was performed using a FACSVantage or FACSAria (Becton–Dickinson).

RNA extraction and real-time quantitative PCR analysis

RNA samples were prepared using silica gel membrane-based spin-columns (RNeasy Mini-KitTM; Qiagen, Valencia, CA) and subjected to reverse transcription (RT) with a Sensiscript-RT Kit (Qiagen). All procedures were performed according to the manufacturer's instructions. For real-time quantitative PCR, primers and the fluorogenic probes were designed and selected according to Roche Universal Primer library software (Roche Diagnostics) and MGB probe system (Applied Biosystems, Carlsbad, CA). The instrument used was the Applied Biosystems ABIPrism 7900HT sequence detection system, and the software for data collection and analysis was SDS2.3. A GAPDH RNA probe (Hs00266705_g1) was used to normalise the data.

Clonogenic colony-forming assay

At the indicated days of culture, from days 6 through 25, the adherent cells were treated with dispase and harvested. They were incubated in a new tissue-culture dish (#3003, Becton–Dickinson) for 10 min to eliminate adherent non-haematopoietic cells [40]. Floating cells were collected and dispersed by 40-μm strainers. After dead cells were eliminated by labeling with Dead-Cert Nanoparticles (#DC-001, ImmunoSolv, Edinburgh, UK), live hematopoietic cells were cultured at a concentration of 1×10^3 (for counting CFU-G) or 10^4 (for counting CFU-Mix, BFU-E, and CFU-GM) cells/ml in 35-mm petri dishes (#1008; Becton-Dickinson) using

1 ml/dish of MethoCult GF+ semisolid medium (#4435; STEMCELL Technologies) as previously described. Colonies were counted after 14–21 days of incubation, and colony types were determined according to the criteria described previously [41,42,43] by in situ observation using an inverted microscope. The abbreviations used for the clonogenic progenitor cells are as follows: CFU-Mix, mixed colony-forming units; BFU-E, erythroid burst-forming units; CFU-GM, granulocyte–macrophage colony-forming units; and CFU-G, granulocyte colony-forming units.

Single-cell deposition assay

The single-cell deposition assay was performed as described previously [17,18,28][17,18,28][17,18,28][17,18,28][17,18,28][17,18,28][17,18,28][17,18,28][17,18,28][17,18,28][17,18,28][17,18,28][17,18,28][17,18,28][17,18,28][17,18,28][17,18,28][17,18,28][17,18,28]. In brief, single sorted cells were deposited in individual wells of 96-well plates with confluent OP9 layers and cultured for 14 days. Wells were scored by morphological observation for hematopoietic colony detection and stained with anti-vascular endothelial cadherin (VE-cadherin) antibodies for endothelial lineage detection.

Chemotaxis assay

Chemotaxis assay was performed with modified Boyden chamber method using 3.0-μm pore size cell culture inserts (Becton Dickinson). In brief, 5×10^4 cells harvested from floating cell fraction at day 25 were added to the upper chamber and induced to migrate towards the lower chamber containing 10 nM formyl-Met-Leu-Phe (fMLP; Sigma-Aldrich) for 4 hours at 37°C. After incubation, the cells in the lower chamber were collected and counted using a MACSQuant flow cytometer (Miltenyi Biotec). For quantitative analysis, equivalent amount of 6-μm beads (Becton Dickinson) were added to each FCM sample, and the cell numbers were determined by measuring the ratio of cells to beads.

Phagocytosis and detection of reactive oxygen species

Phagocytosis and production of reactive oxygen species were detected by chemiluminescent microspheres (luminol-binding carboxyl hydrophilic microspheres; TORAY, Tokyo, Japan) as described previously [44]. In brief, 2×10^4 floating cells were suspended in 50 μL of the reaction buffer (HBSS containing 20 mM *N*-2-hydroxyethylpiperazine-*N*-2-ethanesulfonic acid (HEPES)) per tube. To activate the system, 5 μl chemiluminescent microspheres were added, and light emission was recorded continuously using a luminometer (TD-20/20; Turner Designs, Sunnyvale, CA). During the measurement, samples were kept at 37°C. To inhibit the reaction, 1.75 μg of cytochalasin B (Sigma-Aldrich) was added to the samples.

Measurement of oxygen-binding ability

Floating blood cells derived from KhES-1 and 253G4 strains were harvested on day 32 of differentiation (with erythropoietic cytokine cocktail). Oxygen dissociation curves for hemoglobin were measured using a Hemox-Analyzer (TCS Scientific Corporation, New Hope, PA) as previously reported [45,46].

Results

Stepwise generation of functional hematopoietic cells from human ES/iPS cells in the serum-free monolayer culture without animal-derived stromal cells

To assess the differentiation activity of each human ES/iPS cell line with high reproducibility, we used a chemically defined medium in the monolayer differentiation culture and succeeded in inducing various blood cells, including erythrocytes and neutrophils (Figure 1a). To present the developmental process from human ES/iPS cells to blood cells in an orderly manner, we divided the entire process into 3 steps: (1) initial differentiation into PS cells, (2) induction of the hematopoietic mesoderm (Movie S1), and (3) commitment to the hematopoietic lineages (Movie S2).

Step 1: Induction of PS-like cells from undifferentiated human ES/iPS cells with BMP4 (days 0–4). First, we examined the efficacy of initial progression from undifferentiated pluripotent cells (KhES-1) into PS-like cells according to the expression of representative marker genes, such as *T* and *Mixl1* (Figure 1b), and the change in morphology (Figure 1c). Without cytokines, these genes were only slightly upregulated during the first 4 days. However, when 40 ng/mL BMP4 was added to the culture, the expression levels of these genes increased, which is compatible with previous reports on the importance of BMP4 in mesodermal/endodermal differentiation via PS during early embryogenesis (Figure 1b). Further, transcription levels of the undifferentiated marker *Nanog* decreased. During this period, the colonies showed substantial morphological changes at the margins, and cell density decreased and cell contact diminished (Movie S1, Figure 1c). Immunohistochemical staining assays confirmed the upregulation of T and the lateral mesodermal marker, KDR, and downregulation of Oct3/4 (Figure 1c). However, regarding ectodermal commitment, the representative marker gene *Sox1* was hardly detected on day 4 in the presence of BMP4 (Figure 1b).

To assess the role of BMP4 in this step, we analyzed the differentiation efficacy of individual ES (KhES-1 and KhES-3) and iPS (201B7 and 253G4) cell strains with various concentrations of BMP4 in the presence or absence of its inhibitor, Noggin. As shown in Figure 1d, *T* gene expression was upregulated by BMP4 dose-dependently up to 20 ng/mL and was almost completely suppressed by the BMP4 inhibitor, Noggin, in both ES and iPS cells. This suggested that BMP4 was critical at this stage. From these results, we used BMP4 at 20 ng/mL concentration in subsequent experiments.

We also assayed the expression of several cell surface protein markers in this step (Figure 1e). On day 4, undifferentiated cell markers (TRA-1-60 and SSEA4) were downregulated, whereas paraxial and lateral mesoderm cell markers (CD140a and KDR) and markers for mesodermal and hematopoietic progenitors (CXCR4 and CD117) were upregulated. The early-phase hematopoietic-committed cell markers (CD34 and CD43) were still negative at this stage. Similar results were obtained for both ES and iPS cells (data not shown), suggesting that our system initiated paraxial and lateral mesodermal differentiation from pluripotent stem cells during Step 1 [33].

Step 2: Generation of $KDR^+CD34^+CD45^-$ progenitors with VEGF and SCF (days 4–6). Our previous studies of primate ES cells demonstrated that $KDR^+CD34^+CD45^-$ mesodermal progenitors derived in a VEGF-containing culture on OP9 stromal cells included hematopoietic progenitors [17,18]. Therefore, we used this data to induce these progenitors in our culture system. Considering the partial expression of KDR and CD117 during the first step, we replaced BMP4 with 40 ng/mL $VEGF_{165}$ (ligand for KDR) and 50 ng/mL SCF (ligand for CD117) on day 4 to accelerate selective differentiation to the lateral mesoderm with hematopoietic activities (Figure 1a).

During the next 2 days, the colonies exhibited 2 distinct regions: a plateau-like central area with stratified components and a surrounding area with monolayer cells (Movie S1, Figure 1c). On day 6, the mRNA expression pattern indicated the dominance of mesodermal cells rather than endodermal or ectodermal lineages

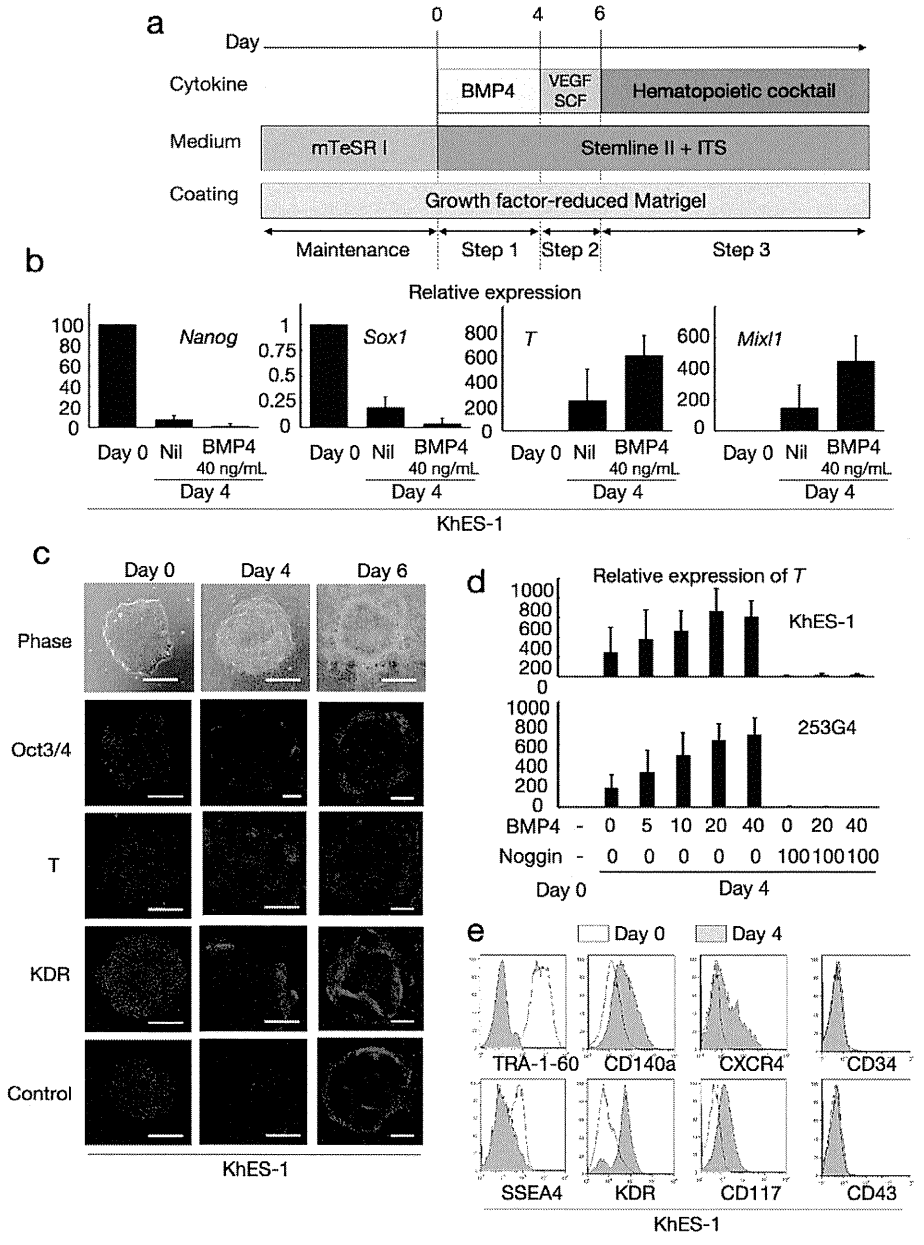

Figure 1. Blood cell induction from pluripotent stem cells starts with commitment into primitive streak. a. A schema of stepwise haematopoietic differentiation of human ES/iPS cells. **b.** Gene expression analysis of colonies at the beginning of differentiation (day 0) and the end of step 1 (day 4) with/without 40 ng/mL BMP4. Data from KhES-1 are shown as representative. **c.** Phase contrast microscopies and immunofluorescence staining of colonies during initial differentiation. Data from KhES-1 are shown as representative. **d.** Relative expression of *T* at day 4 of differentiation with different combinations of BMP4 and its inhibitor Noggin. Where shown, bars represent standard deviation of the mean of three independent experiments; Scale bars, 500 μm. Data from KhES-1 and 253G4 strains are shown as representative. **e.** Flow cytometric analysis of differentiating cells on day 4, indicating the down-regulation of immature cell markers and up-regulation of differentiated progenitor markers. Data from KhES-1 are shown as representative.
doi:10.1371/journal.pone.0022261.g001

(Figure 2a), and flow cytometric (FCM) analysis demonstrated the emergence of new cell fractions that were positive for KDR, CD117, CXCR4, and CD34 but negative for CD140a, CD43, and CD45 (Figure 2b). Our system robustly supports mesodermal induction from both ES and iPS cells, despite differences in efficacy among cell strains (Figure 2c).

Further, immunohistochemical staining for KDR indicated an uneven distribution of KDR^+ cells at the marginal zone of the plateau area (Figure 1c), suggesting that differentiation polarity within the colonies resulted in site-specific emergence of putative hematopoietic mesodermal progenitors.

Step 3: Production of functional blood cells dependent on cytokine cocktails (day 6 onward). On day 6, we changed the culture medium to another chemically defined medium containing hematopoietic cytokines (Figure 1a). To achieve lineage-directed differentiation, we used 2 combinations of cytokines: a myeloid-

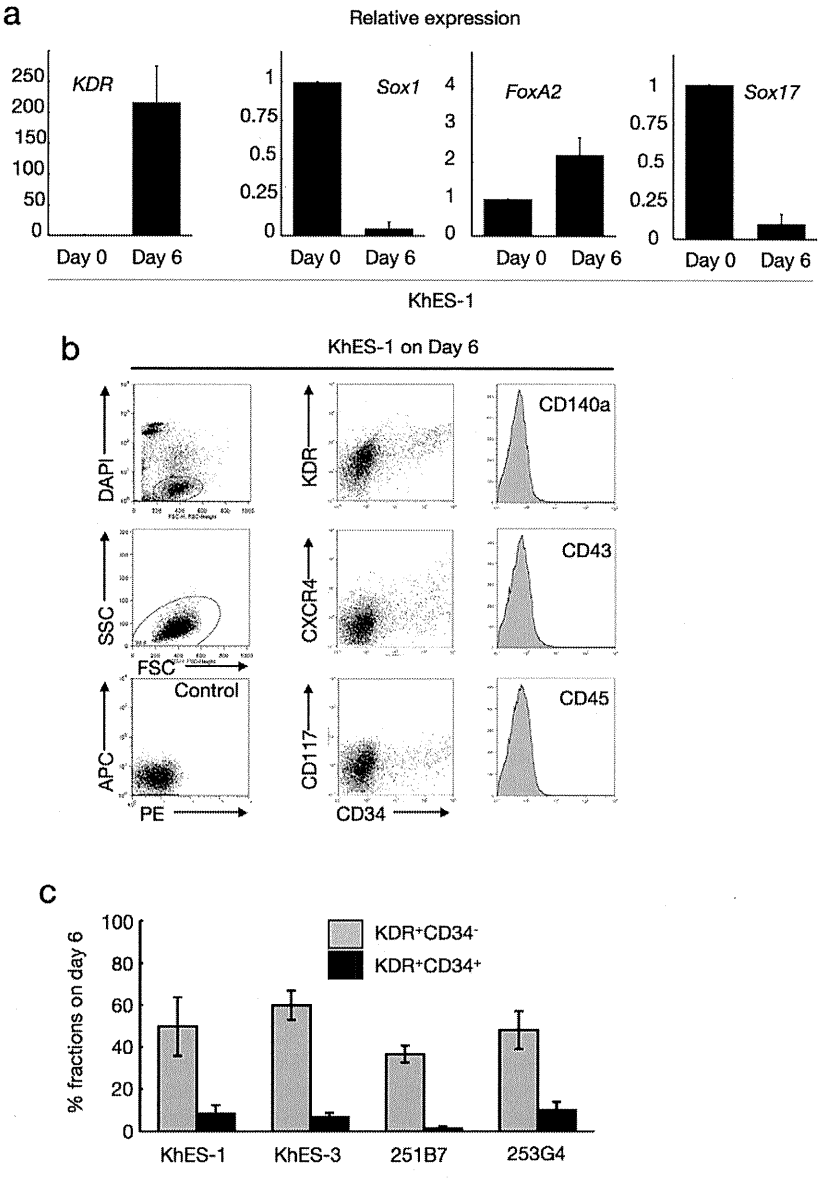

Figure 2. Characterization of cells during initial differentiation with lineage-specific marker expression. a. Expression analysis of lineage-specific marker genes at the beginning of differentiation (day 0) and the end of step 2 (day 6). Bars represent standard deviation of the mean of three independent experiments. Data from KhES-1 are shown as representative. **b.** The development of progenitors on day 6 positive for lateral mesoderm markers but negative for paraxial mesoderm and haematopoietic cell markers. Leftmost column shows the gating strategy for eliminating dead cells and debris. Data from KhES-1 are shown as representative. c. Efficacy of inducing $KDR^{+}CD34^{+\text{ or }-}$ mesodermal progenitors from each two lines of human ES cells and iPS cells. Bars represent standard deviation of the mean of three independent experiments.
doi:10.1371/journal.pone.0022261.g002

induction cocktail containing SCF, TPO, IL3, FLT-3 ligand, and G-CSF; and an erythropoietic-differentiation cocktail containing SCF, TPO, IL3, FP6, and EPO.

Regardless of the cocktails, the colonies first exhibited a rosary-like appearance, with small sac-like structures aligned along the margins of the plateau areas, and grew for several days (Figure 3a, left panel). Hematopoietic cell clusters emerged from the edge of these structures on days 10–12, followed by the appearance of floating blood cells a few days later, which increased thereafter; hematopoietic clusters grew in size and number, and some exhibited areas with a cobblestone-like appearance (Figure 3a, right 3 panels; Movie S2). When fresh medium with the cytokines was supplied every 5 days, blood cell production was observed in both ES and iPS cell experiments until day 50 of differentiation, whereas few hematopoietic cells appeared without the cytokines (data not shown).

As expected, the myeloid-induction cocktail induced myelo-monocytic lineages predominantly positive for CD45. Blood cells harvested on day 30 exhibited morphology compatible with myelomonocytic precursors and mature neutrophils, and displayed positive myeloperoxidase staining (Figure 3b). On the other hand, the erythropoietic-differentiation cocktail yielded cell lineages that included hemoglobin-positive (Hb^{+}) erythroid cells and $CD41^{+}$ megakaryocytes (Figure 3b). In the KhES-1 strain (3.5 [standard deviation (SD) = 1.5] undifferentiated colonies 250 μmm in diameter were initially plated in individual wells of 6-well plates

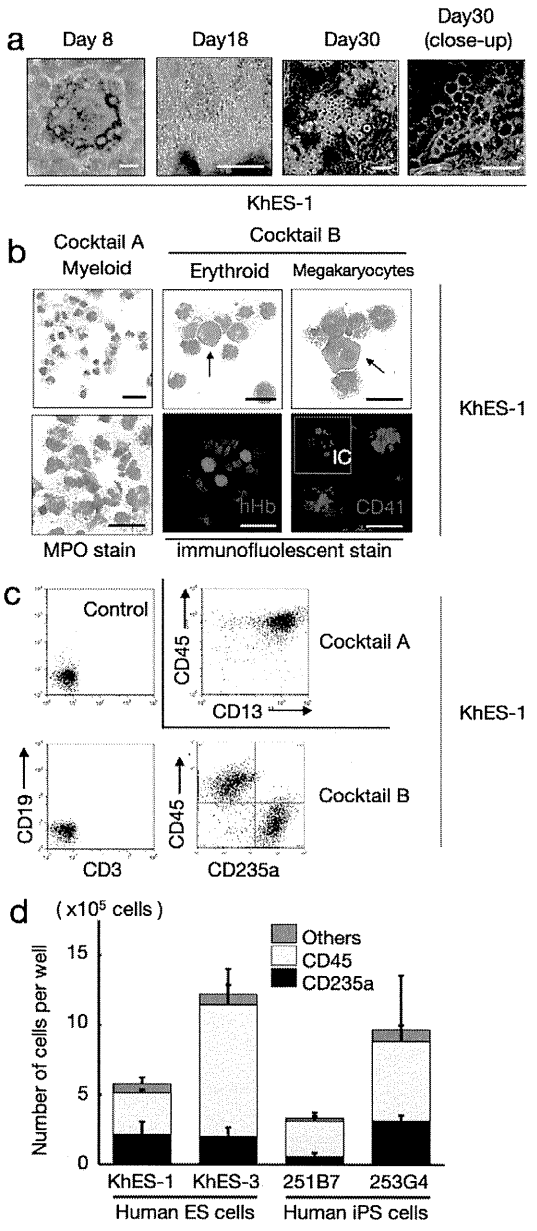

Figure 3. Human ES/iPS cell-derived haematopoiesis in a monolayer culture free from animal serum or stromal cells. a. Sequential phase contrast pictures showing haematopoietic development. Scale bars, 500 μm (left two panels) and 100 μm (right two panels). Data from KhES-1 are shown as representative. **b.** Floating cells harvested on day 30 showing various lineages of haematopoietic cells; MPO-positive myeloid lineage cells (leftmost panels), pan-human Hb-positive erythroid lineage cells (centre panels), and CD41-positive megakaryocytes (rightmost panels). Scale bars, 100 μm. Data from KhES-1 are shown as representative. **c.** Expression of lineage-specific antigens on floating cells harvested on day 30; Myeloid lineages (CD13 and CD45), erythroid lineages (CD235a), T cells (CD3), and B cells (CD19). Data from KhES-1 are shown as representative. **d.** Numbers and fraction of blood cells induced from each two lines of human ES cells and iPS cells. Bars represent standard deviation of the mean of three independent experiments.
doi:10.1371/journal.pone.0022261.g003

at the start of differentiation), counting and FCM analysis of harvested blood cells on day 30 revealed the existence of 7.7×10^5 (SD = 2.3×10^5) different cell lineages per well, including 36.0% (SD = 6.4%) $CD235a^+$ erythroid and 53.2% (SD = 9.4%) $CD45^+$ myelomonocytic lineages, but no lymphoid lineage cells (Figure 3c). Although the differentiation efficacy and lineage distribution depend not only on the cytokines but also on the cell strains, the data indicates that human ES and iPS cells develop into various lineages of hematopoietic cells, robustly and orderly, in our novel monolayer culture system without xeno-derived serum or stromal cells (Figure 3d).

ES/iPS cell-derived hematopoietic cells have similar potential to in vivo-derived blood cells in function

Considering the use of ES/iPS cell-derived hematopoiesis for various clinical and research applications, it is important to confirm the function of the generated blood cells. Neutrophils derived with the myeloid-induction cocktail exhibited migration activity in response to the chemoattractant fMLP (Figure 4a) and phagosome-dependent reactive oxygen production, which was inhibited by the phagosome destruction agent, cytochalasin B (Figure 4b). On the other hand, erythroid lineage cells derived with the erythropoietic-differentiation cocktail (harvested on day 32 of differentiation) exhibited an oxygen dissociation curve that was similar, despite being slightly left-shifted, to those obtained with adult and cord blood cells (Figure 4c). These data indicate that our culture facilitates robust and orderly development of human ES and iPS cells into functional hematopoietic cells with similar potential to in vivo-derived blood cells.

Clonogenic hematopoietic development from human ES/iPS cell-derived progenitors

The human hematopoietic system is a hierarchy of various component cells from stem or progenitor cells to terminally differentiated cells. For example, $CD34^+$ cells in umbilical cord blood or bone marrow contain putative hematopoietic stem cells and are used as a source of stem cell transplantation. The identification and proliferation of such cells in vitro have been of great interest in medical science research.

To assess the potential of our system for supporting generated immature stem or progenitor cells, we evaluated the colony-forming ability of the cultivated hematopoietic progenitors in the system. Accordingly, the cells were cultured with SCF, TPO, IL3, FLT-3 ligand, and FP6. In these conditions, $CD34^+CD45^+$ hematopoietic cells existed up to day 25, indicating that the immature hematopoietic cells can be maintained in our serum-free culture (Figure 5a).

We harvested adherent blood cells from the previously described culture and transferred them into a methylcellulose-containing medium to perform colony-forming assays with SCF, TPO, IL3, G-CSF, and EPO. As shown in Figure 5b and c, CFU-Mix, BFU-E, CFU-GM, and CFU-G colonies developed from plated cells. The total number of colonies increased dramatically from day 6 to day 10, then gradually increased until day 15 and decreased thereafter. CFU-Mix and BFU-E colonies were mainly observed until day 15 and were thereafter replaced by CFU-GM and CFU-G colonies. Similar tendencies were observed in both ES and iPS cells. These results suggest that our culture system can incubate multipotent hematopoietic stem or progenitor cells over a period of time.

Identification of $KDR^+CD34^+CD45^-$ bipotential hemoangiogenic progenitors derived in serum-free conditions

During embryogenesis, hematopoietic development is closely associated with endothelial lineage commitment [47,48], and

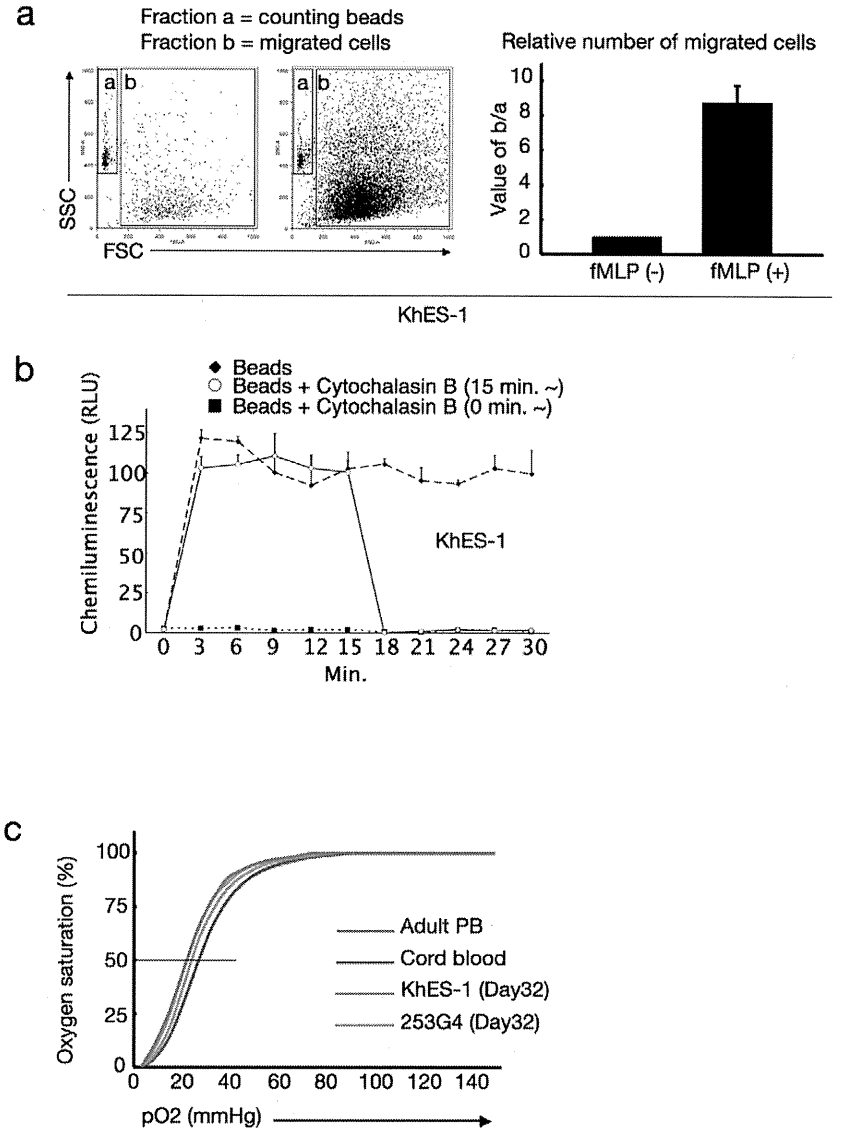

Figure 4. Functional blood cells derived from human ES/iPS cells. a. Number of migrated cells that permeated through the transwell membrane with or without fMLP. Values were normalised to the number of counting beads, and the control values were arbitrarily set to the condition without fMLP. Data from KhES-1 are shown as representative. **b.** Assay for phagocytosis-induced respiratory burst activity using chemiluminescent microspheres (luminol-binding microspheres). Abbreviation: RLU, relative light units. Data from KhES-1 are shown as representative. **c.** Oxygen dissociation curves of erythroid cells derived from human ES/iPS cells (harvested on day32 of differentiation), human cord blood, and adult peripheral blood. Where shown, bars represent standard deviation of the mean of three independent experiments.
doi:10.1371/journal.pone.0022261.g004

previous studies have demonstrated that ES cells can differentiate into the common multipotent progenitors that differentiate into both blood and endothelial cells at the single cell level on OP9 stroma [17,28,49]. Although the experiments described thus far demonstrated that the serum-free, xeno-cell-free culture condition supported human ES/iPS cell-derived hematopoiesis in an orderly manner, as observed during embryogenesis, it was unclear which day 6 fraction(s) developed into blood cells. To clarify this point, human ES cells stably expressing green fluorescent protein (GFP) were cultured, then 1×10^4 cells of $GFP^+KDR^-CD34^-CD45^-$ (Fraction A), $GFP^+KDR^+CD34^-CD45^-$ (Fraction B), and $GFP^+KDR^+CD34^+CD45^-$ (Fraction C) fractions were transferred on day 6 into a synchronous differentiation culture of unlabeled ES cells (Figure 6a). Nineteen days later (day 25 of differentiation), GFP^+ small round cell-containing colonies were observed predominantly in Fractions B and C, and FCM analysis of the entire culture confirmed the emergence of GFP^+CD45^+ cells mainly from Fraction C (Figure 6b). On the other hand, few blood cells positive for GFP were generated from Fraction A. These results were obtained with 2 independent strains of human ES cells (KhES1-EGFPneo on KhES-1 and KhES3-EGFPneo on KhES-3) (Figure 6c) and indicated that hematopoietic progenitors were present in the KDR^+ fraction, particularly in the KDR^+CD34^+ fraction, on day 6 of differentiation.

Finally, we performed a single-cell deposition assay by transferring single sorted human ES/iPS cell-derived $GFP^+KDR^+CD34^+CD45^-$ cells, which were negative for VE-cadherin, on day 6 into individual wells of 96-well plates coated

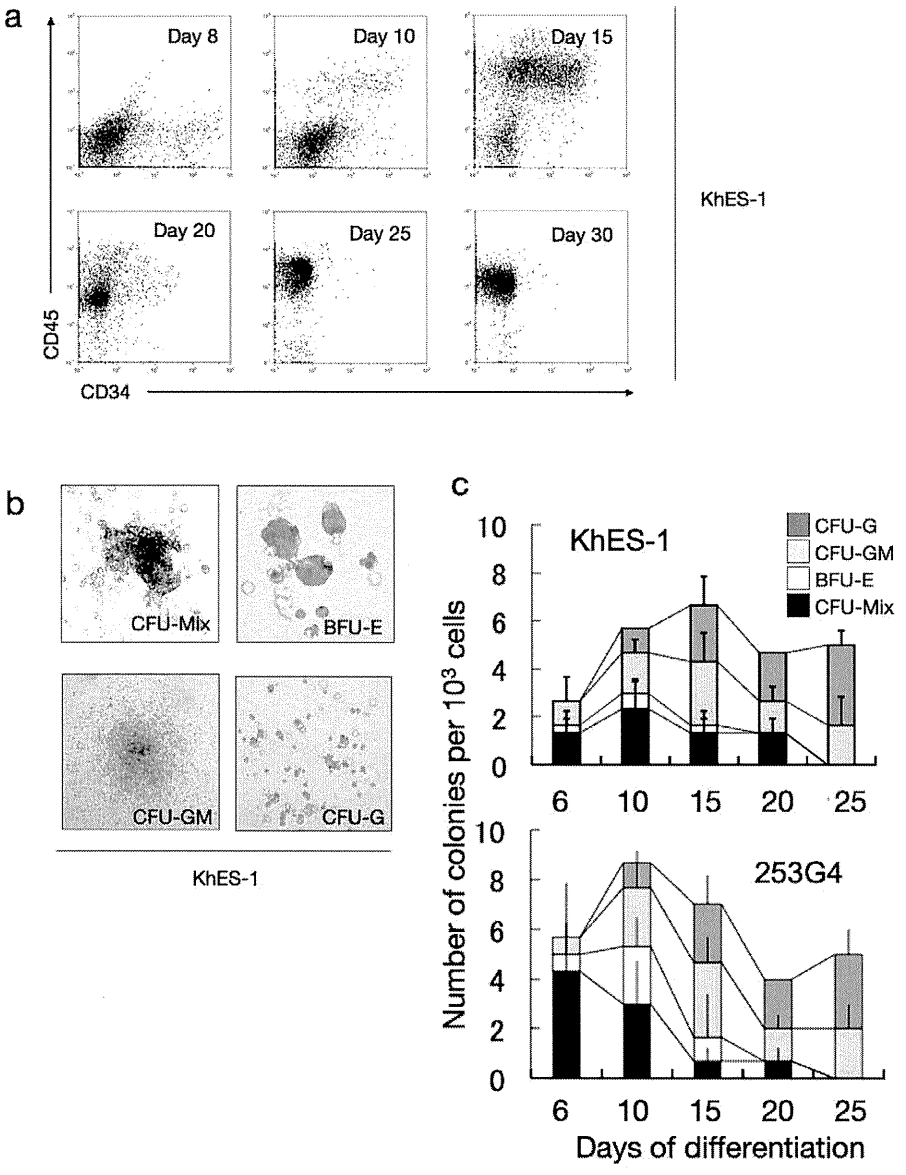

Figure 5. Hematopoietic stem/progenitor cells in culture. a. Sequential FCM analysis of cells harvested on indicated days showing the existence of $CD34^{+}CD45^{+}$ haematopoietic progenitor cells in culture. Data from KhES-1 are shown as representative. **b.** Various colony types on MTC-containing medium clonally emerged from single haematopoietic progenitor cells. Data from KhES-1 are shown as representative. **c.** Numbers of each colony type derived from different days of culture. Bars represent standard deviation of the mean of three independent experiments. Data from KhES-1 and 253G4 strains are shown as representative.
doi:10.1371/journal.pone.0022261.g005

with an OP9 cell layer. As shown in Figure 6d and e, the proportion of hematopoietic cell (HC) development, VE-cadherin^{+} endothelial cell (EC) development, and HC plus EC development on day 20 were 9.0%, 6.8%, and 4.0%, respectively, for KhES-1 and 11.6%, 12.7%, and 8.3%, respectively, for 253G4 iPS cells. These results demonstrate that the common mesodermal progenitors that can differentiate into both blood and endothelial cells at the single-cell level are induced in our culture condition.

Discussion

In this study, we demonstrated the orderly mesodermal and hematopoietic differentiation of human ES and iPS cells in a novel serum-free monolayer culture condition. Simple manipulation of cytokine combinations facilitated robust, reproducible, and highly directed stepwise commitment to specific lineages of functional blood cells.

There are several reports on hematopoietic differentiation of human ES/iPS cells, such as murine-derived OP9 stromal cell coculture and feeder/serum-free EB formation systems [20,22,23,24,30,31,32,50]. However, two-dimensional cultures containing xeno-serum/cells often cause dependency on their lots, while complicated three-dimensional structures inside EBs make it difficult to assess and control conditions for inducing specific progenitors. Actually, few in vitro systems have been able to reliably reproduce hematopoietic development from mesodermal progenitors or model the in vivo coexistence of developing hematopoietic cells and their autologous microenvironments in

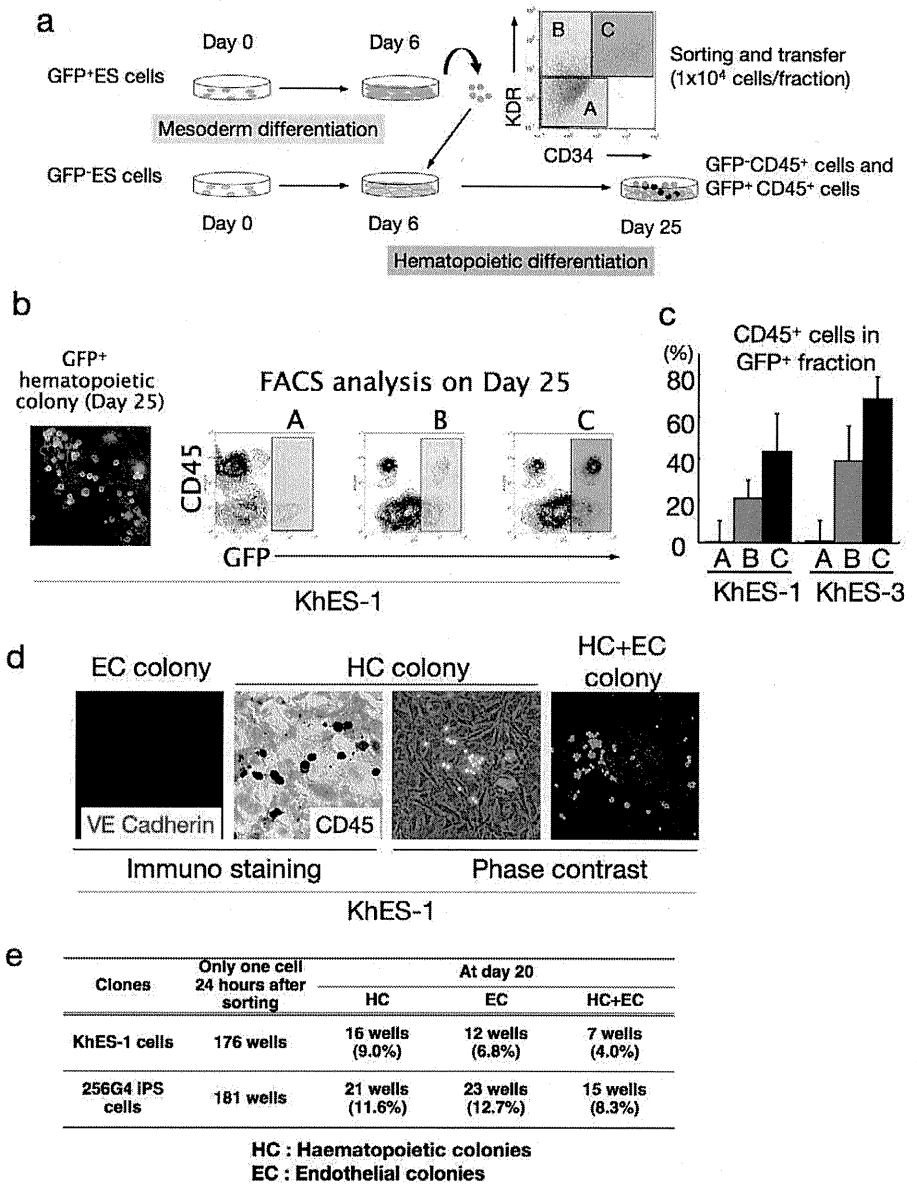

e

Clones	Only one cell 24 hours after sorting	At day 20		
		HC	EC	HC+EC
KhES-1 cells	176 wells	16 wells (9.0%)	12 wells (6.8%)	7 wells (4.0%)
256G4 IPS cells	181 wells	21 wells (11.6%)	23 wells (12.7%)	15 wells (8.3%)

HC : Haematopoietic colonies
EC : Endothelial colonies

Figure 6. Haematopoietic differentiation from KDR$^+$CD34$^+$ mesodermal progenitors. a. Schema of the protocol for measuring haematopoietic activities of depicted fractions on day 6. **b.** Each sorted fraction-derived haematopoiesis on day 25 detected by fluorescent microscopy and FCM analysis. Data from KhES-1 are shown as representative. **c.** Ratio of CD45$^+$ cells in GFP$^+$ fraction on day 25 showing the strongest haematopoietic activity of fraction C followed by fraction B. **d.** Single KDR$^+$CD34$^+$CD45$^-$ cell-derived haematopoietic colonies (HC), VE-cadherin$^+$ endothelial colonies (EC), and HC+EC colonies generated on OP9 cell layers. Data from KhES-1 are shown as representative. **e.** Number of wells that showed HC, EC, and EC+HC development.
doi:10.1371/journal.pone.0022261.g006

serum-free conditions. Our less labor-intensive and clearly defined monolayer culture facilitates observation of the stepwise development of pluripotent cells to blood cells via common hemoangiogenic progenitors and the behavior of hematopoietic cells on autologous stromal cells. Consequently, assays for elucidating differences in lineage specification of various ES/iPS cell strains, including hematopoietic potential, can be performed with high reproducibility. This is particularly important because individual pluripotent cell strains vary in differentiation potentials [51,52,53]. This study demonstrated quantitative differences in hematopoietic differentiation efficacy and lineage commitment among 4 ES/iPS cell strains.

Because human ES/iPS cells are feasible cell sources for various clinical applications, scientific and medical communities have shown continuing interest in hematopoietic stem cell induction from ES/iPS cells. Previous trials have indicated that murine ES cell-derived hematopoietic cells overexpressing HoxB4 [54] can replenish the bone marrow of lethally irradiated recipient mice. However, it remains a challenge to develop bona fide human hematopoietic stem cells with bone marrow reconstitution activity at the single-cell level. In our study, we observed many cobblestone area-forming cells, which reportedly indicate the existence of very immature hematopoietic progenitors. Moreover, FCM analyses and colony-forming assays suggested that ES and iPS human cell-

derived hematopoiesis in our method occurs through clonogenic hematopoietic stem/progenitor cells. We are in the process of determining in vivo repopulating ability of cells harvested from our culture by using serial transplantation into immunodeficient mice to assess the possibility of inducing feasible cell sources for various clinical applications, such as cell therapies and disease investigation.

Finally, time-lapse imaging strongly indicated crosstalk between hematopoietic cells and the autologous microenvironment composed of non-hematopoietic cells. Emerged blood cells move about actively and generate colonies in surrounding cell layers, suggesting the importance of a direct interaction between blood cells and microenvironmental cells for the maintenance, proliferation, and differentiation of stem or progenitor cells (Movie S3). In fact, a model of hematopoietic disorders triggered by mutation in the bone marrow microenvironment has been recently reported [55]. However, further investigation is necessary to identify the mechanisms responsible for such phenomena. Our culture may aid these investigations as it facilitates simple and sequential harvest of hematopoietic cells with minimal contamination by autologous adherent cell layers.

In conclusion, this study presents novel methods for analyzing the mechanisms of normal hematopoiesis in a robust, reproducible, and stepwise manner. Furthermore, employing gene-manipulated ES cells or disease-specific iPS cells will supply in vitro models of disease pathology, thereby providing further insights into hematological defects in conditions such as aplastic anemia and myelodysplastic syndromes.

Supporting Information

Movie S1 Time-lapse microscopic movie showing the morphological change in a single colony from day 0 to day 6 (initial differentiation). In this period, a colony begins forming a rosary-like morphology as it differentiates. The pictures were automatically taken every 8 minute by Biostation IM (Nikon Instruments, Tokyo, Japan).
(MOV)

Movie S2 Time-lapse microscopic movie showing the morphological change in a single colony from day 6 to day 25 (hematopoietic differentiation). After adding hematopoietic cytokines on day 6, hematopoietic cells first emerge from the areas near the edge of stratified zone. The pictures were automatically taken every 8 minute by Biostation IM (Nikon Instruments, Tokyo, Japan).
(MOV)

Movie S3 Close-up time-lapse microscopic movie showing hematopoietic cells moving about and generating colonies in surrounding cell layers. The pictures were automatically taken every 8 minute by Biostation IM (Nikon Instruments, Tokyo, Japan).
(MOV)

Acknowledgments

We are grateful to Kyowa Hakko Kirin Co. Ltd. for providing FP6. We thank N. Nakatsuji (Institute for Frontier Medical Sciences, Kyoto University) for providing human ES cells and S. Yamanaka (CiRA) for providing human iPS cells. We thank T. Tanaka (Nakahata-ken, CiRA) for his advice on undifferentiated human ES/iPS cell culture; T. Morishima (Graduate school of medicine, Kyoto University) for instructing the function assay of neutrophils; Y. Sasaki, S. Tomida, M. Yamane, and Y. Shima (Nakahata-ken, CiRA) for their excellent technical assistance; and H. Koyanagi (Nakahata-ken, CiRA), N. Hirakawa, Y. Ogihara, and G. Odani (Nikon Instruments Company) for their expertise in microscopic time-lapse monitoring. We thank H. Watanabe (Nakahata-ken, CiRA), M. Muraki, M. Terada, H. Konishi, C. Kaji, N. Takasu, and Y. Takao (Kenkyu-Senryaku-honbu, CiRA) for their superb administrative assistance.

Author Contributions

Conceived and designed the experiments: AN TH KU TN MKS. Performed the experiments: AN H. Sakai. Analyzed the data: AN TH KU KO IK H. Sakai. TN MKS. Contributed reagents/materials/analysis tools: H. Suemori H. Sakai. Wrote the manuscript: AN TN MKS.

References

1. Evans MJ, Kaufman MH (1981) Establishment in culture of pluripotential cells from mouse embryos. Nature 292: 154–156.
2. Thomson JA, Itskovitz-Eldor J, Shapiro SS, Waknitz MA, Swiergiel JJ, et al. (1998) Embryonic stem cell lines derived from human blastocysts. Science 282: 1145–1147.
3. Keller G (2005) Embryonic stem cell differentiation: emergence of a new era in biology and medicine. Genes Dev 19: 1129–1155.
4. Xu Y, Shi Y, Ding S (2008) A chemical approach to stem-cell biology and regenerative medicine. Nature 453: 338–344.
5. Shi Y, Do JT, Desponts C, Hahm HS, Scholer HR, et al. (2008) A combined chemical and genetic approach for the generation of induced pluripotent stem cells. Cell Stem Cell 2: 525–528.
6. Jaenisch R, Young R (2008) Stem cells, the molecular circuitry of pluripotency and nuclear reprogramming. Cell 132: 567–582.
7. Meissner A, Wernig M, Jaenisch R (2007) Direct reprogramming of genetically unmodified fibroblasts into pluripotent stem cells. Nat Biotechnol 25: 1177–1181.
8. Garcia-Porrero JA, Manaia A, Jimeno J, Lasky LL, Dieterlen-Lievre F, et al. (1998) Antigenic profiles of endothelial and hemopoietic lineages in murine intraembryonic hemogenic sites. Dev Comp Immunol 22: 303–319.
9. Choi K, Kennedy M, Kazarov A, Papadimitriou JC, Keller G (1998) A common precursor for hematopoietic and endothelial cells. Development 125: 725–732.
10. Wood HB, May G, Healy L, Enver T, Morriss-Kay GM (1997) CD34 expression patterns during early mouse development are related to modes of blood vessel formation and reveal additional sites of hematopoiesis. Blood 90: 2300–2311.
11. Shalaby F, Ho J, Stanford WL, Fischer KD, Schuh AC, et al. (1997) A requirement for Flk1 in primitive and definitive hematopoiesis and vasculogenesis. Cell 89: 981–990.
12. Sumi T, Tsuneyoshi N, Nakatsuji N, Suemori H (2008) Defining early lineage specification of human embryonic stem cells by the orchestrated balance of canonical Wnt/beta-catenin, Activin/Nodal and BMP signaling. Development 135: 2969–2979.
13. Flamme I, Breier G, Risau W (1995) Vascular endothelial growth factor (VEGF) and VEGF receptor 2 (flk-1) are expressed during vasculogenesis and vascular differentiation in the quail embryo. Dev Biol 169: 699–712.
14. Risau W (1995) Differentiation of endothelium. FASEB J 9: 926–933.
15. Risau W, Hallmann R, Albrecht U (1986) Differentiation-dependent expression of proteins in brain endothelium during development of the blood-brain barrier. Dev Biol 117: 537–545.
16. Huber TL, Kouskoff V, Fehling HJ, Palis J, Keller G (2004) Haemangioblast commitment is initiated in the primitive streak of the mouse embryo. Nature 432: 625–630.
17. Umeda K, Heike T, Yoshimoto M, Shiota M, Suemori H, et al. (2004) Development of primitive and definitive hematopoiesis from nonhuman primate embryonic stem cells in vitro. Development 131: 1869–1879.
18. Umeda K, Heike T, Yoshimoto M, Shinoda G, Shiota M, et al. (2006) Identification and characterization of hemoangiogenic progenitors during cynomolgus monkey embryonic stem cell differentiation. Stem Cells 24: 1348–1358.
19. Ji P, Jayapal SR, Lodish HF (2008) Enucleation of cultured mouse fetal erythroblasts requires Rac GTPases and mDia2. Nat Cell Biol 10: 314–321.
20. Vodyanik MA, Bork JA, Thomson JA, Slukvin II (2005) Human embryonic stem cell-derived CD34+ cells: efficient production in the coculture with OP9 stromal cells and analysis of lymphohematopoietic potential. Blood 105: 617–626.
21. Kitajima K, Tanaka M, Zheng J, Yen H, Sato A, et al. (2006) Redirecting differentiation of hematopoietic progenitors by a transcription factor, GATA-2. Blood 107: 1857–1863.
22. Takayama N, Nishikii H, Usui J, Tsukui H, Sawaguchi A, et al. (2008) Generation of functional platelets from human embryonic stem cells in vitro via ES-sacs, VEGF-promoted structures that concentrate hematopoietic progenitors. Blood 111: 5298–5306.

23. Choi KD, Vodyanik MA, Slukvin II (2009) Generation of mature human myelomonocytic cells through expansion and differentiation of pluripotent stem cell-derived lin-CD34+CD43+CD45+ progenitors. J Clin Invest 119: 2818–2829.
24. Choi KD, Yu J, Smuga-Otto K, Salvagiotto G, Rehrauer W, et al. (2009) Hematopoietic and endothelial differentiation of human induced pluripotent stem cells. Stem Cells 27: 559–567.
25. Niwa A, Umeda K, Chang H, Saito M, Okita K, et al. (2009) Orderly hematopoietic development of induced pluripotent stem cells via Flk-1(+) hemoangiogenic progenitors. J Cell Physiol 221: 367–377.
26. Timmermans F, Velghe I, Vanwalleghem L, De Smedt M, Van Coppernolle S, et al. (2009) Generation of T cells from human embryonic stem cell-derived hematopoietic zones. J Immunol 182: 6879–6888.
27. Morishima T, Watanabe K, Niwa A, Fujino H, Matsubara H, et al. (2011) Neutrophil differentiation from human-induced pluripotent stem cells. J Cell Physiol 226: 1283–1291.
28. Shinoda G, Umeda K, Heike T, Arai M, Niwa A, et al. (2007) alpha4-Integrin(+) endothelium derived from primate embryonic stem cells generates primitive and definitive hematopoietic cells. Blood 109: 2406–2415.
29. Ji J, Vijayaragavan K, Bosse M, Menendez P, Weisel K, et al. (2008) OP9 stroma augments survival of hematopoietic precursors and progenitors during hematopoietic differentiation from human embryonic stem cells. Stem Cells 26: 2485–2495.
30. Chadwick K, Wang L, Li L, Menendez P, Murdoch B, et al. (2003) Cytokines and BMP-4 promote hematopoietic differentiation of human embryonic stem cells. Blood 102: 906–915.
31. Wang L, Li L, Shojaei F, Levac K, Cerdan C, et al. (2004) Endothelial and hematopoietic cell fate of human embryonic stem cells originates from primitive endothelium with hemangioblastic properties. Immunity 21: 31–41.
32. Wang L, Menendez P, Shojaei F, Li L, Mazurier F, et al. (2005) Generation of hematopoietic repopulating cells from human embryonic stem cells independent of ectopic HOXB4 expression. J Exp Med 201: 1603–1614.
33. Nostro MC, Cheng X, Keller GM, Gadue P (2008) Wnt, activin, and BMP signaling regulate distinct stages in the developmental pathway from embryonic stem cells to blood. Cell Stem Cell 2: 60–71.
34. Gadue P, Huber TL, Paddison PJ, Keller GM (2006) Wnt and TGF-beta signaling are required for the induction of an in vitro model of primitive streak formation using embryonic stem cells. Proc Natl Acad Sci U S A 103: 16806–16811.
35. Kennedy M, D'Souza SL, Lynch-Kattman M, Schwantz S, Keller G (2007) Development of the hemangioblast defines the onset of hematopoiesis in human ES cell differentiation cultures. Blood 109: 2679–2687.
36. Martin R, Lahlil R, Damert A, Miquerol L, Nagy A, et al. (2004) SCL interacts with VEGF to suppress apoptosis at the onset of hematopoiesis. Development 131: 693–702.
37. Grigoriadis AE, Kennedy M, Bozec A, Brunton F, Stenbeck G, et al. (2010) Directed differentiation of hematopoietic precursors and functional osteoclasts from human ES and iPS cells. Blood 115: 2769–2776.
38. Takahashi K, Tanabe K, Ohnuki M, Narita M, Ichisaka T, et al. (2007) Induction of pluripotent stem cells from adult human fibroblasts by defined factors. Cell 131: 861–872.
39. Suemori H, Yasuchika K, Hasegawa K, Fujioka T, Tsuneyoshi N, et al. (2006) Efficient establishment of human embryonic stem cell lines and long-term maintenance with stable karyotype by enzymatic bulk passage. Biochem Biophys Res Commun 345: 926–932.
40. Suwabe N, Takahashi S, Nakano T, Yamamoto M (1998) GATA-1 regulates growth and differentiation of definitive erythroid lineage cells during in vitro ES cell differentiation. Blood 92: 4108–4118.
41. Nakahata T, Ogawa M (1982) Hemopoietic colony-forming cells in umbilical cord blood with extensive capability to generate mono- and multipotential hemopoietic progenitors. J Clin Invest 70: 1324–1328.
42. Nakahata T, Ogawa M (1982) Identification in culture of a class of hemopoietic colony-forming units with extensive capability to self-renew and generate multipotential hemopoietic colonies. Proc Natl Acad Sci U S A 79: 3843–3847.
43. Nakahata T, Spicer SS, Ogawa M (1982) Clonal origin of human erythro-eosinophilic colonies in culture. Blood 59: 857–864.
44. Uchida T, Kanno T, Hosaka S (1985) Direct measurement of phagosomal reactive oxygen by luminol-binding microspheres. J Immunol Methods 77: 55–61.
45. Ma F, Ebihara Y, Umeda K, Sakai H, Hanada S, et al. (2008) Generation of functional erythrocytes from human embryonic stem cell-derived definitive hematopoiesis. Proc Natl Acad Sci U S A 105: 13087–13092.
46. Fujimi A, Matsunaga T, Kobune M, Kawano Y, Nagaya T, et al. (2008) Ex vivo large-scale generation of human red blood cells from cord blood CD34+ cells by co-culturing with macrophages. Int J Hematol 87: 339–350.
47. Yamaguchi TP, Dumont DJ, Conlon RA, Breitman ML, Rossant J (1993) flk-1, an flt-related receptor tyrosine kinase is an early marker for endothelial cell precursors. Development 118: 489–498.
48. Asahara T, Murohara T, Sullivan A, Silver M, van der Zee R, et al. (1997) Isolation of putative progenitor endothelial cells for angiogenesis. Science 275: 964–967.
49. Kennedy M, Firpo M, Choi K, Wall C, Robertson S, et al. (1997) A common precursor for primitive erythropoiesis and definitive haematopoiesis. Nature 386: 488–493.
50. Grigoriadis AE, Kennedy M, Bozec A, Brunton F, Stenbeck G, et al. (2010) Directed differentiation of hematopoietic precursors and functional osteoclasts from human ES and iPS cells. Blood 115: 2769–2776.
51. Kim K, Doi A, Wen B, Ng K, Zhao R, et al. (2010) Epigenetic memory in induced pluripotent stem cells. Nature 467: 285–290.
52. Osafune K, Caron L, Borowiak M, Martinez RJ, Fitz-Gerald CS, et al. (2008) Marked differences in differentiation propensity among human embryonic stem cell lines. Nat Biotechnol 26: 313–315.
53. Ji H, Ehrlich LI, Seita J, Murakami P, Doi A, et al. (2010) Comprehensive methylome map of lineage commitment from haematopoietic progenitors. Nature 467: 338–342.
54. Kyba M, Perlingeiro RC, Daley GQ (2002) HoxB4 confers definitive lymphoid-myeloid engraftment potential on embryonic stem cell and yolk sac hematopoietic progenitors. Cell 109: 29–37.
55. Raaijmakers MH, Mukherjee S, Guo S, Zhang S, Kobayashi T, et al. (2010) Bone progenitor dysfunction induces myelodysplasia and secondary leukaemia. Nature 464: 852–857.

Journal of Cellular Physiology

Neutrophil Differentiation From Human-Induced Pluripotent Stem Cells

TATSUYA MORISHIMA,[1] KEN-ICHIRO WATANABE,[1] AKIRA NIWA,[2] HISANORI FUJINO,[1] HIROSHI MATSUBARA,[1] SOUICHI ADACHI,[1] HIROFUMI SUEMORI,[3] TATSUTOSHI NAKAHATA,[2] AND TOSHIO HEIKE[1]*

[1]*Department of Pediatrics, Graduate School of Medicine, Kyoto University, Kyoto, Japan*

[2]*Department of Clinical Application, Center for iPS Cell Research and Application, Kyoto University, Kyoto, Japan*

[3]*Laboratory of Embryonic Stem Cell Research, Stem Cell Research Center, Institute for Frontier Medical Sciences, Kyoto University, Kyoto, Japan*

Induced pluripotent stem (iPS) cells are of potential value not only for regenerative medicine, but also for disease investigation. The present study describes the development of a neutrophil differentiation system from human iPS cells (hiPSCs) and the analysis of neutrophil function and differentiation. The culture system used consisted of the transfer of hiPSCs onto OP9 cells and their culture with vascular endothelial growth factor (VEGF). After 10 days, TRA 1-85^{+}CD34^{+}VEGF receptor-2 (VEGFR-2)^{high} cells were sorted and co-cultured with OP9 cells in the presence of hematopoietic cytokines for 30 days. Floating cells were collected and subjected to morphological and functional analysis. These hiPSC-derived neutrophils were similar to peripheral blood mature neutrophils in morphology, contained functional neutrophil specific granules, and were equipped with the basic functions such as phagocytosis, superoxide production, and chemotaxis. In the process of differentiation, myeloid cells appeared sequentially from immature myeloblasts to mature segmented neutrophils. Expression patterns of surface antigen, transcription factors, and granule proteins during differentiation were also similar to those of granulopoiesis in normal bone marrow. In conclusion, differentiation of mature neutrophils from hiPSCs was successfully induced in a similar process to normal granulopoiesis using an OP9 co-culture system. This system may be applied to elucidate the pathogenesis of various hematological diseases that affect neutrophils.

J. Cell. Physiol. 226: 1283–1291, 2011.

Neutrophils and/or myeloid differentiation are most commonly affected in various hematological diseases including inherited bone marrow failure syndromes and neutrophil function disorders. Responsible genes have been identified in most of these syndromes or diseases, but the association between the gene mutation and the specific phenotype is not always clear. Moreover, often patients who present with a specific syndrome lack mutations in the known genes (Alter, 2007). Understanding the pathophysiology of these syndromes has been challenging despite the information provided by recent molecular findings, and in many of these syndromes, experimental models have not yet been generated.

Murine models of human congenital and acquired diseases are invaluable for disease investigation, but they provide a limited representation of human pathophysiology because they often do not faithfully mimic human diseases. The differences between murine and human physiologies make human cell culture an essential complement to research with animal models of disease.

Induced pluripotent stem (iPS) cells are reprogrammed somatic cells with embryonic stem (ES) cell-like characteristics generated by the introduction of combinations of specific transcription factors (Takahashi and Yamanaka, 2006; Meissner et al., 2007; Okita et al., 2007; Takahashi et al., 2007; Yu et al., 2007; Park et al., 2008b). Given the robustness of the approach, direct reprogramming promises to be a facile source of patient-derived cell lines. Such lines would be immediately valuable not only for regenerative medicine, but for disease investigation and drug screening as well.

The pluripotency and self-renewal potential of ES cells contributes to their value in various fields of science (Evans and Kaufman, 1981). Previous studies using normal or gene-manipulated ES cells have helped elucidate the process of normal embryogenesis and the genetic mechanisms of certain diseases (Lensch and Daley, 2006; Tulpule et al., 2010). Use of human embryos, however, faces ethical controversies that hinder the applications of human ES cells (hESCs). In addition, it is difficult to generate patient- or disease-specific ES cells, which are required for their effective application. The use of iPS cells would avoid the controversies surrounding human embryonic stem cell research.

Patient-specific iPS cells can be used for the generation of disease-corrected, patient-specific cells for cell therapy applications. Disease-specific pluripotent cells capable of differentiation into the various tissues affected in each condition can also provide new insights into disease pathophysiology by permitting analysis in a human system, under controlled conditions in vitro. Recent studies reported the generation of disease-specific iPS cell lines from patients with a variety of diseases (Park et al., 2008a; Raya et al., 2009; Agarwal et al., 2010). Therefore, disease-specific iPS cells are expected to be good models for the investigation of different diseases, and

Contract grant sponsor: The Ministry of Education, Culture, Sports, Science and Technology, Japan.

*Correspondence to: Toshio Heike, Department of Pediatrics, Graduate School of Medicine, Kyoto University, 54 Kawahara-cho, Shogoin, Sakyo-ku, Kyoto 606-8507, Japan.
E-mail: heike@kuhp.kyoto-u.ac.jp

Received 21 May 2010; Accepted 20 September 2010

Published online in Wiley Online Library (wileyonlinelibrary.com), 13 October 2010.
DOI: 10.1002/jcp.22456

effective neutrophil differentiation systems are required to investigate the pathogenesis of various hematological conditions that affect neutrophils using human iPS cells (hiPSCs).

Recent reports describe in vitro culture systems for neutrophil differentiation from hESCs (Choi et al., 2009; Saeki et al., 2009; Yokoyama et al., 2009); however, neutrophil differentiation from hiPSCs has not yet been reported in detail. One of these studies demonstrated that myeloid differentiation could be induced from hiPSCs using the same methodology employed for their differentiation from hESCs (Choi et al., 2009), but the differentiation process and the functions of hiPSC-derived neutrophils were not shown in detail. A system for erythroid differentiation from primate ES and murine iPS cells by co-culture with OP9 stromal cells was developed in previous studies (Umeda et al., 2004; Umeda et al., 2006; Shinoda et al., 2007; Niwa et al., 2009). In the present study, a neutrophil differentiation system from hiPSCs was established by modifying the erythroid differentiation system, and the functions of the hiPSC-derived neutrophils and their differentiation process were analyzed in detail. This system may contribute to the elucidation of the pathogenesis of various blood diseases and the development of novel therapeutic approaches.

Materials and Methods

Maintenance of cells

The human iPS cell lines 201B6, 253G1 and 253G4 were a kind gift from Dr. Yamanaka (Kyoto University, Kyoto), and were generated from human dermal fibroblasts by retrovirus-mediated transfection of four (201B6) or three (253G1 and 253G4) transcription factors (Oct3/4, Sox2, and Klf4, with or without c-Myc) (Takahashi et al., 2007; Nakagawa et al., 2008). The human iPS cell lines and the human ES cell line KhES3-EGFPneo (KhES-3G) were maintained on mitomycin-C (Kyowa Hakko Kirin, Tokyo, Japan) -treated mouse embryonic fibroblasts (MEFs) in DMEM/F12 (Sigma-Aldrich, St. Louis, MO) supplemented with 20% Knockout™ Serum Replacement (Invitrogen, Carlsbad, CA), 5 ng/ml basic fibroblast growth factor (bFGF; R&D Systems, Minneapolis, MN), 1% non-essential amino acids solution (Invitrogen), 5 mM sodium hydroxide solution, 100 μM 2-mercaptethanol, and 2 mM L-glutamine. The culture medium was replaced daily with fresh medium. Colonies were passaged onto new MEFs every 3 or 4 days. The human ES cell line was used in conformity with The Guidelines for Derivation and Utilization of Human Embryonic Stem Cells of the Ministry of Education, Culture, Sports, Science, and Technology, Japan. OP9 stromal cells, which were a kind gift from Dr. Kodama (Osaka University, Osaka), were maintained in α-MEM (Invitrogen) supplemented with 20% fetal calf serum (FCS; Biological Industries, Bet Haemek, Israel).

Antibodies

The antibodies used for flow cytometric analysis included fluorescein isothiocyanate (FITC)-conjugated anti-human TRA 1-85 (R&D Systems), CD45 (Becton-Dickinson, Franklin Lakes, NJ) antibodies, phycoerythrin (PE)-conjugated anti-human CD11b, CD34 (Beckman Coulter, Fullerton, CA), CD13, CD16, CD33 (Becton-Dickinson) antibodies, and allophycocyanin (APC)-conjugated anti-human vascular endothelial growth factor receptor-2 (VEGFR-2) (eBioscience, San Diego, CA) antibody. The primary antibodies used for immunocytochemical analysis included goat anti-human lactoferrin (Santa Cruz Biotechnology, Santa Cruz, CA) and rabbit anti-human MMP9 (Abcam, Cambridge, UK). Biotinylated horse anti-goat or anti-rabbit antibodies (Vector Laboratories, Burlingame, CA) were used as secondary antibodies.

Differentiation of iPS cells

Methods used for the initial differentiation of iPS cells and cell sorting were based on earlier reports (Umeda et al., 2004, 2006). Briefly, trypsin-treated undifferentiated iPS cells were transferred onto OP9 cells and cultured with 20 ng/ml vascular endothelial growth factor (VEGF) (R&D Systems). After 10 days, the induced cells were harvested with cell dissociation buffer (Invitrogen), and sorted TRA 1-85^{+}CD34^{+}VEGFR-2^{high} cells were transferred onto fresh OP9 cells in six-well plates at a concentration of 3×10^{3} cells per well. Sorted cells were cultured in α-MEM (Invitrogen) containing 10% FCS (Sigma, St Louis, MO), 50 μM 2-mercaptoethanol, 20 ng/ml interleukin (IL)-3, 100 ng/ml stem cell factor (SCF) (R&D Systems), and 10 ng/ml thrombopoietin (TPO) for 20 days. On day 20 after cell sorting, cytokines were changed into 20 ng/ml IL-3 and 10 ng/ml granulocyte colony-stimulating factor (G-CSF). IL-3, TPO and G-CSF were kindly provided by Kyowa Hakko Kirin.

Flow cytometric analysis and cell sorting

Cells were trypsinized and stained with antibodies. Dead cells were excluded by 4',6-diamidino-2-phenylindole (DAPI) staining. Samples were analyzed using an LSR flow cytometer and Cell Quest software (Becton Dickinson). Cell sorting was performed using a FACSVantage SE flow cytometer (Becton Dickinson).

Cytostaining

Floating cells were centrifuged onto glass slides using a Shandon Cytospin® 4 Cytocentrifuge (Thermo, Pittsburgh, PA), and analyzed by microscopy after May–Giemsa, myeloperoxidase (MPO), or alkaline-phosphatase staining. Sequential morphological analysis was performed as follows: all adherent cells including OP9 cells were trypsinized, harvested, and incubated in a new tissue-culture dish (Becton-Dickinson) for 1 h to eliminate adherent OP9 cells (Suwabe et al., 1998). Floating cells were then collected, centrifuged onto glass slides, and analyzed by microscopy after May–Giemsa staining. For immunocytochemical analysis, cells were fixed with 4% paraformaldehyde (PFA), immersed in citrate buffer, and autoclaved for 5 min at 121°C for antigen retrieval (Toda et al., 1999). The slides were then incubated with primary antibodies followed by application of the streptavidinbiotin complex immunoperoxidase technique with diaminobenzidine as chromogen, and nuclei were counterstained with hematoxylin.

Electron microscopy

Cells were fixed in 2% glutaraldehyde in 0.1 M phosphate buffer (PB) for at least 2 h, and then postfixed in 1% osmium tetroxide in 0.1 M PB for 1.5 h. After fixation, samples were dehydrated in a graded ethanol series, cleared with propylene oxide, and embedded in Epon. Thin sections of cured samples were stained with uranyl acetate and Reynolds lead citrate. The sections were inspected using a transmission electron microscope, H7650 (Hitachi, Tokyo, Japan).

Chemotaxis assay

Chemotactic ability was determined using a modified Boyden chamber method (Boyden, 1962; Harvath et al., 1980). Briefly, 500 μl of the reaction medium (Hank's Balanced Salt Solution (HBSS) containing 2.5% FCS) with or without 10 nM formyl-Met-Leu-Phe (fMLP; Sigma-Aldrich) was placed into each well of a 24-well plate, and the cell culture insert (3.0-μm pores; Becton Dickinson) was gently placed into each well to divide the well into upper and lower sections. Floating cells were suspended in the reaction medium at 7.0×10^{4}/ml, and a 500-μl cell suspension was added to the upper well, allowing the cells to migrate from the upper to the lower side of the membrane for 4 h at 37°C. After incubation, cells in the lower chamber were collected and counted using an LSR flow cytometer. Cells were counted by flow cytometry as follows:

equivalent amounts of counting beads were added to each sample and counted until the bead count reached 10,000.

MPO activity assay

The EnzChek Myeloperoxidase (MPO) Activity Assay Kit (Molecular Probes, Leiden, The Netherlands) was used for rapid and sensitive determination of MPO chlorination activity in cell lysates. The procedure was performed following the manufacturer's instructions. Cell lysate samples were prepared from 1×10^4 floating cells by freeze-thaw cycles. Fluorescence was measured with a fluorescence microplate reader (Wallac 1420 ARVO sx; PerkinElmer, Waltham, MA) using fluorescence excitation and emission at 485 and 530 nm, respectively. The background fluorescence measured for each zero-MPO control reaction was subtracted from each fluorescence measurement before plotting.

DHR assay

Neutrophil production of reactive oxygen species was detected by flow cytometry using dihydrorhodamine123 (DHR) as described previously (Vowells et al., 1995). Briefly, 3.5×10^4 floating cells were suspended in 100 μl of the reaction buffer (HBSS containing 0.1% FCS and 5 mM glucose) per tube, and two tubes were prepared for each sample. Catalase (Sigma-Aldrich) at a final concentration of 1000 U/ml and DHR at a final concentration of 1.0×10^5 nM were added and incubated for 5 min in a 37°C shaking water bath. After incubation, phorbol myristate acetate (PMA; Sigma-Aldrich) at a final concentration of 400 ng/ml was added to one of the two tubes and tubes were returned to the water bath for an additional 15 min. Following incubation, rhodamine fluorescence from the oxidized DHR was detected using an LSR flow cytometer.

Phagocytosis and detection of reactive oxygen species

Phagocytosis and neutrophil production of reactive oxygen species was detected by chemiluminescent microspheres (luminol-binding carboxyl hydrophilic microspheres; TORAY, Tokyo, Japan) as described previously (Uchida et al., 1985). Briefly, 2×10^4 floating cells were suspended in 50 μl of the reaction buffer (HBSS containing 20 mM N-2-hydroxyethylpiperazine-N′-2-ethanesulfonic acid (HEPES)) per tube. To activate the system, 5 μl of chemiluminescent microspheres was added, and light emission was recorded continuously. During the measurement, samples were kept at 37°C. To inhibit the phagocytosis, 1.75 μg of cytochalasin B (Sigma-Aldrich) was added to the sample. Chemiluminescence from the microspheres was detected using a luminometer (TD-20/20; Turner Designs, Sunnyvale, CA).

RNA extraction and RT-PCR analysis

RNA samples were prepared using silica gel membrane-based spin-columns (RNeasy Mini-Kit™, Qiagen, Valencia, CA) and subjected to reverse transcription (RT) with the Ominscript-RT Kit™ (Qiagen). All procedures were performed following the manufacturer's instructions. For reverse transcriptase-polymerase chain reaction (RT-PCR), yields were adjusted by dilution to produce equal amounts of the human glyceraldehyde-3-phosphate dehydrogenase (GAPDH) amplicon. The complementary DNA (cDNA) templates were initially denatured at 94°C for 5 min, followed by 30–40 amplification reactions consisting of 94°C for 15–30 sec (denaturing), 55–63°C for 15–30 sec (annealing), and 72°C for 30–60 sec (extension), with a final extension at 72°C for 7 min. The oligonucleotide primers were as follows: NANOG, 5′-CAG CCC TGA TTC TTC CAC CAG TCC C-3′ and 5′-TGG AAG GTT CCC AGT CGG GTT CAC C-3′ (Takahashi et al., 2007); human GAPDH, 5′-CAC CAG GGC TGC TTT TAA CTC TG-3′ and 5′-ATG GTT CAC ACC CAT GAC GAA C-3′ (Umeda et al., 2006); PU.1, 5′-CTG CAT TGG CCC CCA CCG AG-3′ and 5′-AGG TCT TCT GAT GGC TGA GGG GG-3′; C/EBPα, 5′-TAA CCT TGT GCC TTG GAA ATG CAA AC-3′ and 5′- ATG TTT CCA CCC CTT TCT AAG GAC A-3′ (Duan and Horwitz, 2003); C/EBPε, 5′- AGT CTG GGG AAG AGC AGC TTC-3′ and 5′- ACA GTG TGC CAC TTG GTA CTG-3′ (Mori et al., 2009); MPO, 5′-TGA GGA CGG CTT CTC TCT TC-3′ and 5′-CCC GGT AAG TGA TGA TCT GG-3′; Lactoferrin, 5′-AGC TGG CAG ACT TTG CGC T-3′ and 5′-TTC AGA TTA GTA ATG CCT GCG ACA TAC-3′ (Kholodnyuk et al., 2006); Gelatinase (MMP-9), 5′-GCC TCC AAC CAC CAC CAC AC-3′ and 5′-GCC CAG CCC ACC TCC ACT C-3′ (Sugimoto et al., 2001); mouse GAPDH, 5′-ACG GCC GCA TCT TCT TGT GCA-3′ and 5′-CAC CCT TCA AGT GGG CCC CG-3′. PCR amplification reaction cycles were performed in the linear range for each primer by carrying out primer titrations. The number of reaction cycles per sample were: NANOG, 35 cycles; human GAPDH, 30 cycles; PU.1, 40 cycles; C/EBPα, 40 cycles; C/EBPε, 40 cycles; MPO, 35 cycles; Lactoferrin, 35 cycles; Gelatinase (MMP-9), 40 cycles; mouse GAPDH, 30 cycles.

Statistics

Statistical analyses were conducted using the Student's *t*-test. Statistical significance was defined as $P < 0.05$.

Results

Neutrophil differentiation from hiPSCs in co-culture with OP9 stromal cells

A culture system for the induction of erythroid cell differentiation from primate ES and murine iPS cells by co-culture with OP9 stromal cells (Umeda et al., 2004; Umeda et al., 2006; Shinoda et al., 2007; Niwa et al., 2009) was established, and this system was applied for neutrophil differentiation from hiPSCs. Prior data in primate ES cells suggested that the VEGFR-2^{high} fraction of differentiated cells contained hemangioblasts and VEGFR-2^{high}CD34$^+$ cells had more hematopoietic potential (Umeda et al., 2006). Therefore, the expression of VEGFR-2 and CD34 was examined using three human iPS cell lines (201B6, 253G1, 253G4) and one ES cell line (KhES-3G). After 10 days of co-culture with OP9 in the presence of 20 ng/ml VEGF, VEGFR-2^{high}CD34$^+$ cells appeared from all hiPSC lines in a similar manner to the ES cell line (Fig. 1A). Among these three human iPS cell lines, the highest percentage of VEGFR-2^{high}CD34$^+$ cells was detected in 253G4 (Fig. 1B), and the data on this cell line is therefore presented below.

The VEGFR-2^{high}CD34$^+$ cell fraction was sorted (Fig. 1C) and 1.1×10^4 (range; 0.6–2.2×10^4 in 14 independent cultures) VEGFR-2^{high}CD34$^+$ cells were grown in one 10-cm dish containing hiPSCs. They were then transferred onto fresh OP9 cells and cultured in the presence of hematopoietic cytokines. Around 10 days after cell sorting (day10 + 10), small, round cell colonies appeared (Fig. 1D), and these colonies gradually grew in both size and number (Fig. 1E). At the same time, floating cells also appeared, and the average number of floating cells from 1×10^4 sorted VEGFR-2^{high}CD34$^+$ cells at 30 days after cell sorting (day10 + 30) was 4.1×10^4 (range; 0.2–9.9×10^4 in 11 independent cultures).

May–Giemsa staining of the floating cells on day 10 + 30 revealed that 38.0 ± 1.6% of the cells were stab and segmented neutrophils (Fig. 1F), which were positive for MPO (Fig. 1G) and neutrophil alkaline-phosphatase (Fig. 1H). The rest were mainly immature myeloid cells and a small number of macrophages, and cells of other lineages, such as erythroid or lymphoid cells, were not observed. The frequency of MPO- and neutrophil alkaline-phosphatase-positive cells is shown in Table 1. The results were consistent with the morphological features revealed by May–Giemsa staining.

Surface marker analysis revealed that these floating cells were positive for CD45 and CD11b, and partially positive for CD13, CD33, and CD16 (Fig. 1I). The expression pattern of these surface markers was similar to that of neutrophils or immature myeloid cells in healthy bone marrow (van Lochem et al., 2004), although the CD16 expression level was lower.

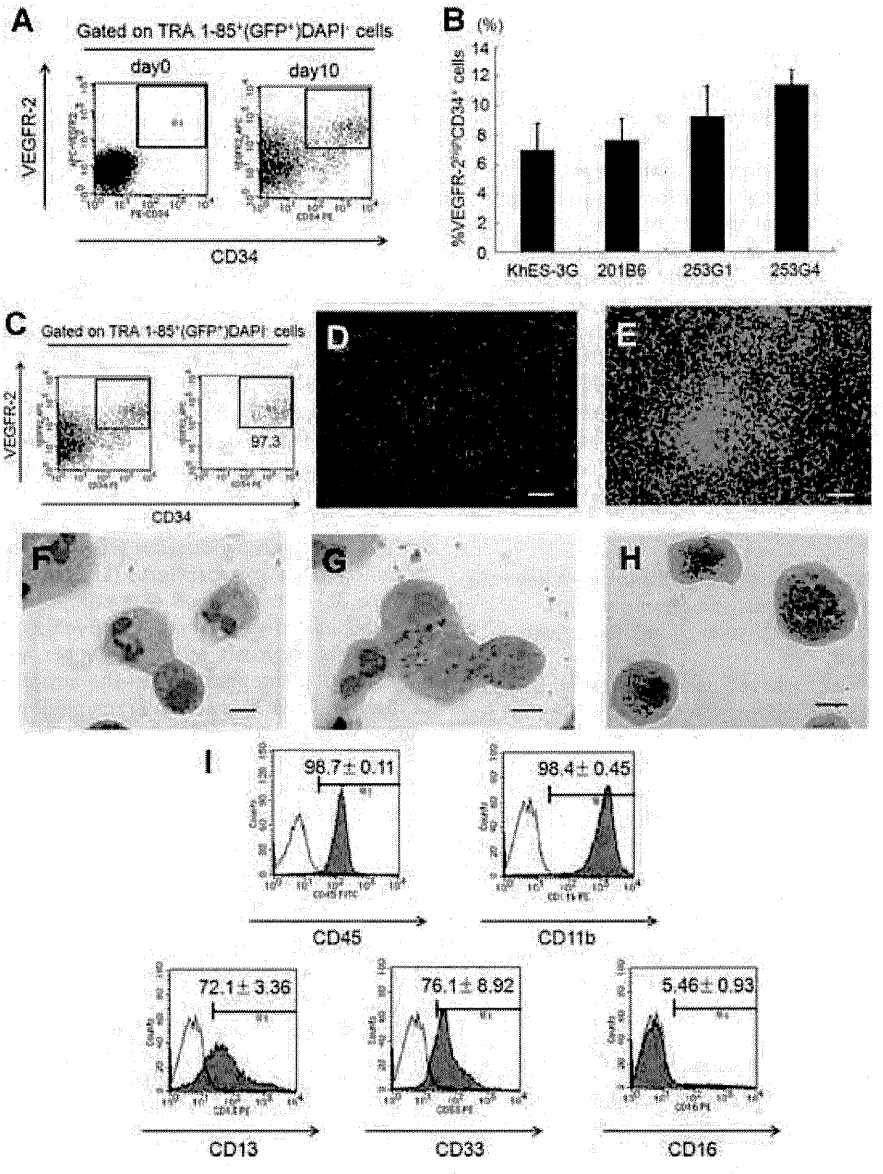

Fig. 1. Neutrophil differentiation from hiPSCs in co-culture with OP9 stromal cells. (A–B) Flow cytometric analysis of VEGFR-2 and CD34 during differentiation induction. TRA 1-85$^+$ (GFP$^+$) DAPI$^-$ cells were gated as human iPS (ES) cell-derived viable cells. Undifferentiated iPS (ES) cells and 10-day culture cells were stained with antibodies specific for VEGFR-2 and CD34. Representative results from one of three independent experiments (A) and percentages of VEGFR-2^{high}CD34$^+$ cells on day 10 (B) are shown (n = 3; bars represent SDs). (C) VEGFR-2^{high}CD34$^+$ cells were sorted on day 10. Representative dot plots and percentages of gated cells are shown. Purities of viable VEGFR-2^{high}CD34$^+$ cells were calculated at 95.5 ± 1.9% from 14 independent experiments. (D–E) Micrographs of adherent hematopoietic cell clusters generated on day 10 (D) and day 30 (E) after cell sorting. Scale bars: 200 μm. (F–H) May–Giemsa staining (F), myeloperoxidase staining (G), and neutrophil alkaline-phosphatase staining (H) of floating cells on day10 + 30. Scale bars: 10 μm. (I) Flow cytometric analysis of floating cells on day10 + 30 were stained with antibodies specific for CD45, CD11b, CD13, CD33, or CD16. Plots show the negative control profile (open bars) versus the specific antibody staining profiles (shaded bars). Representative results from one of three independent experiments are shown. [Color figure can be viewed in the online issue, which is available at wileyonlinelibrary.com.]

TABLE 1. Frequency of staining-positive cells for neutrophil specific granules

Staining	Frequency of positive cells (%)
Myeloperoxidase	93.7 ± 1.7
Neutrophil alkaline-phosphatase	39.0 ± 2.2
Lactoferrin	79.0 ± 1.4
Gelatinase	59.0 ± 3.7

Data are shown as mean ± SD (n = 3 independent experiments).

This lower CD16 expression level was similar to that of neutrophils derived in vitro from bone marrow CD34$^+$ cells by stimulation with G-CSF (Kerst et al., 1993b) and to the effect in vivo when G-CSF is administered to healthy volunteers (Kerst et al., 1993a). These results indicated that the modified OP9 co-culture system could differentiate mature neutrophils from immature hiPSCs.

hiPSC-derived neutrophils contain neutrophil specific granules

Mature neutrophils in vivo have intracellular granules that are important for their bactericidal function. The granules can be

classified into three types based on their size, morphology, or electron density, or with reference to a given protein: primary (azurophilic) granules contain MPO, secondary granules contain lactoferrin, and tertiary granules contain gelatinase (Borregaard and Cowland, 1997).

To assess the presence of these granules in hiPSC-derived neutrophils, they were imaged using transmission electron microscopy, which showed that the hiPSC-derived mature neutrophils contained peroxidase-positive and negative granules, as was observed in peripheral blood neutrophils (Fig. 2A–B). Immunocytochemical analysis revealed that hiPSC-derived mature neutrophils were also positive for lactoferrin and gelatinase (Fig. 2C–D). The frequencies of cells that were positive for neutrophil specific granules, as observed by transmission electron microscopy (Table 2) and immunocytochemical analysis (Table 1), were more than 90% for primary granules, about 80% for secondary granules, and approximately 60% for tertiary granules. These results indicated that hiPSC-derived neutrophils contained neutrophils-specific granules.

hiPSC-derived neutrophils exhibit biological bactericidal activities

Because neutrophils patrol circulating blood and play a key role in early phase defense mechanisms, the chemotactic, phagocytotic, and bactericidal activities of hiPSC-derived neutrophils were analyzed.

Chemotactic activity was assessed using a modified Boyden chamber method (Boyden, 1962; Harvath et al., 1980). After incubation with or without fMLP in the lower well, neutrophils had migrated from the upper side to the lower side of the membrane. Incubation with fMLP caused an increase in the number of migrated cells of more than three times compared to cells without fMLP, suggesting that hiPSC-derived neutrophils had chemotactic activity in response to a chemoattractant similar to natural neutrophils derived from bone marrow (Fig. 3A).

The MPO-dependent chlorination activity and reactive oxygen production of hiPSC-derived neutrophils, which are

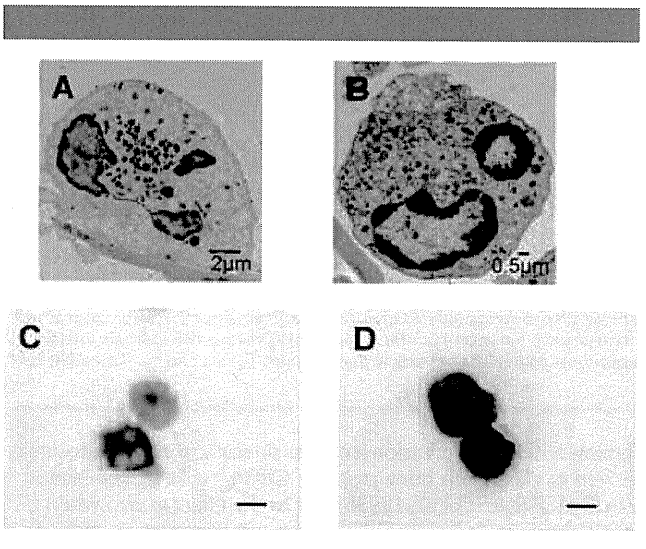

Fig. 2. Neutrophil-specific granules in hiPSC-derived neutrophils. (A–B) Floating cells on day10 + 30 (A) and peripheral blood neutrophils (B) were analyzed by transmission electron microscope. (C–D) Immunocytochemical analysis. Floating cells on day10 + 30 were stained for lactoferrin (C) and MMP9 (gelatinase) (D). Scale bars: 10 μm. [Color figure can be viewed in the online issue, which is available at wileyonlinelibrary.com.]

TABLE 2. Frequency of positive cells for neutrophil specific granules under transmission electron microscopy

Granules	Frequency of positive cells (%)
Peroxidase-positive granules	95.1 (135/142)
Peroxidase-negative granules	86.6 (123/142)

both essential for their bactericidal function, were determined next. MPO reacts with hydrogen peroxide (H_2O_2) to form the active redox and enzyme intermediate compound MPO-I, which oxidizes chloride (Cl^-) to HOCl (Winterbourn, 2002). As shown in Figure 3B, hiPSC-derived neutrophils showed MPO-dependent chlorination activity. To evaluate reactive oxygen production, the ability to convert DHR to rhodamine was assessed using flow cytometry (Vowells et al., 1995) and the results revealed that hiPSC-derived neutrophils characteristically produced superoxide in response to PMA (Fig. 3C).

Finally, phagocytotic activity and phagosome-dependent reactive oxygen production were measured using luminol-bound microspheres (Uchida et al., 1985). As shown in Figure 3D, the captured data confirmed that hiPSC-derived neutrophils could produce reactive oxygen species in response to the phagocytosis of microspheres, which was completely abolished in the presence of the antiphagocytic agent cytochalasin B. Moreover, transmission electron microscopy successfully captured a screenshot of a neutrophil phagocytosing the microbeads (Fig. 3E). The above results clearly show that neutrophils derived from hiPSC using the present culture system maintain their functional status.

Step-wise neutrophil differentiation from hiPSCs is similar to normal granulopoiesis

Disorders of neutrophil differentiation are observed in various hematological diseases, among them the maturation arrest of neutrophil precursors in the bone marrow at the promyelocyte stage in severe congenital neutropenia. Thus, in clinical applications for disease investigation, the sequential analysis of the differentiation process from hiPSC to mature neutrophils in this culture system is required.

Observation of the sequential changes in cell morphology was done using May–Giemsa staining. Visualization of the morphology of day10 + 10 cells revealed that the cells were mainly myeloblasts and promyelocytes (Fig. 4A). On day10 + 20, myelocytes and metamyelocytes became predominant (Fig. 4B), and on day 10 + 30, stab and segmented neutrophils became predominant (Fig. 4C).

Surface antigen expression at each differentiation stage of hiPSC-derived cells was analyzed by flow cytometry (Fig. 4D). CD34, cell surface marker on normal immature hematopoietic cells, was detected in about 20% of the cells on day 10 + 10, but disappeared gradually thereafter. From day 10 + 10 to 10 + 30, the common myeloid antigens CD11b and CD33 were expressed in almost all the cells. Interestingly, expression of CD13, also a common myeloid antigen, was observed in less than 20% of cells at day 10 + 10 and did not subsequently increase. The expression level of CD16, which is a representative marker of matured neutrophils (van de Winkel and Anderson, 1991), doubled from day 10 + 10 to day 10 + 20, although the increase in expression was not statistically significant. These expression patterns were consistent with the patterns observed during normal neutrophil differentiation in healthy bone marrow (van Lochem et al., 2004).

The gene expression patterns of the pluripotency marker, transcription factors and granule proteins during neutrophil

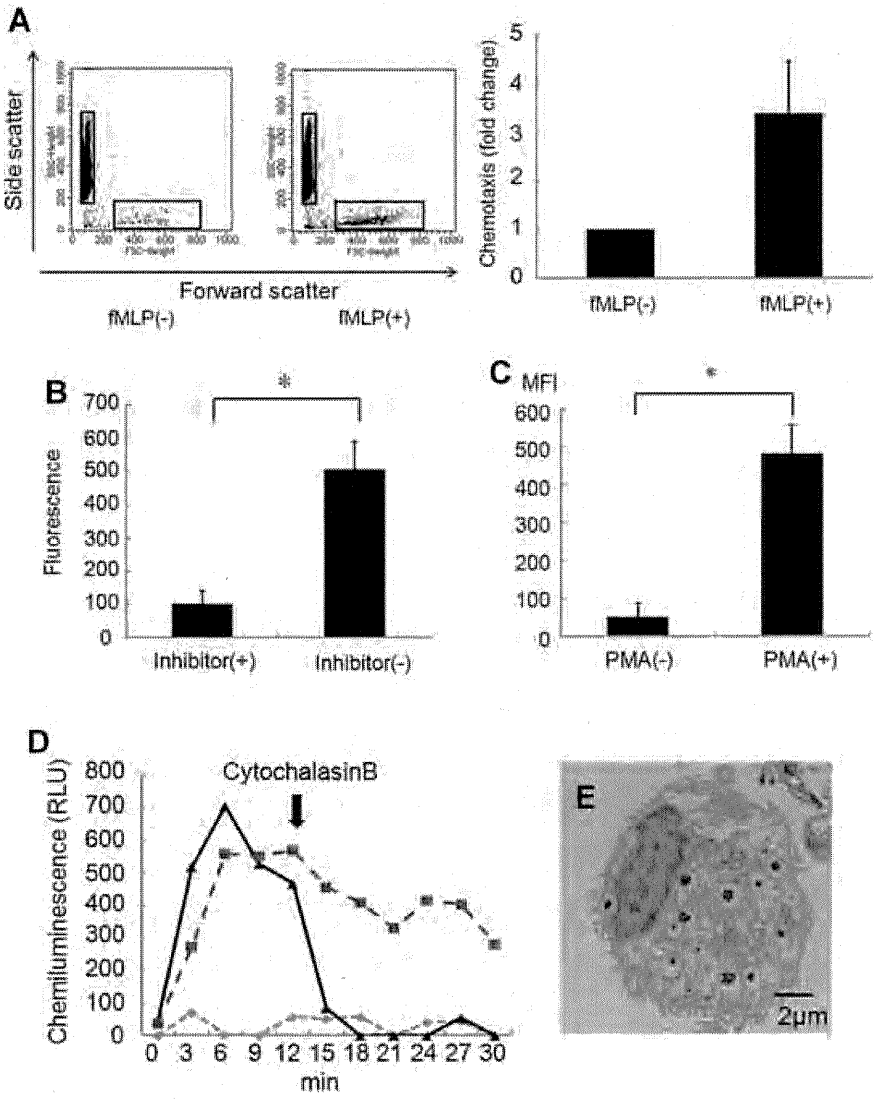

Fig. 3. Functional analysis of hiPSC-derived neutrophils. (A) Chemotactic activity of floating cells on day10 + 30 in response to fMLP was determined as described in Materials and Methods section. After a 4-h culture, the transwell inserts were removed, and the cells in the lower chamber were counted by an LSR flow cytometer (n = 3; bars represent SDs). (B) MPO chlorination activity in cell lysates from floating cells on day10 + 30 was analyzed by EnzChek Myeloperoxidase (MPO) Activity Assay Kit as described in the Materials and Methods section. The chlorination activity in neutrophil cell lysates was almost completely abolished by the addition of a chlorination inhibitor (n = 3; bars represent SDs; *$P < 0.05$.). (C) Floating cells on day10 + 30 were subjected to DHR assay. DHR was reacted with neutrophils with or without PMA, and the resultant rhodamine fluorescence was detected by flow cytometry. The addition of PMA increased the levels of fluorescence. Results are expressed as mean fluorescence intensity (MFI) (n = 3; bars represent SDs; *$P < 0.05$.). (D) Floating cells on day10 + 30 were subjected to the assay for phagocytosis-induced respiratory burst activity using chemiluminescent microspheres (luminol-binding microspheres). Gradual increase in chemiluminescence indicates the respiratory burst triggered by the phagocytosis of luminol-binding microspheres (squares). The increase in chemiluminescence was almost completely abolished by the addition of cytochalasin B (diamonds) and inhibited by its later addition (triangles). The figures are representative of three independent experiments. Abbreviation: RLU, relative light units. (E) hiPSC-derived neutrophils phagocytosing the microbeads were analyzed by transmission electron microscopy.

differentiation in this culture system were investigated by RT-PCR (Fig. 4E–F). NANOG, a pluripotency marker, was expressed in undifferentiated iPS cells but disappeared in sorted VEGFR2^{high}CD34^{+} cells after 10 days differentiation. PU.1 and C/EBPα, essential transcription factors for commitment and differentiation of the granulocytic lineage (Borregaard et al., 2001; Friedman, 2007) were first detected on day 10 + 10 and persisted thereafter. C/EBPε, which had a critical role for the later stages of neutrophil development and transcription of key granule proteins (Borregaard et al., 2001; Friedman, 2007) were first detected faintly on day 10 + 10 and upregulated thereafter. MPO and lactoferrin, which were expressed at the highest levels in myeloblasts/promyelocytes and myelocytes/metamyelocytes, respectively (Cowland and Borregaard, 1999; Borregaard et al., 2001), were detected on day 10 + 10. Gelatinase, which was expressed at the highest level in band and segmented neutrophilic cells (Cowland and Borregaard, 1999; Borregaard et al., 2001), was first detected on day 10 + 20 and upregulated thereafter. Altogether, these results suggested that the neutrophil differentiation in this co-culture system might recapitulate the orderly differentiation process in bone marrow.